TRITA-CSC-A 2009:14
ISSN 1653-5723
ISBN 978-91-7155-901-2

KTH School of Computer Science and Communication
SE-100 44 Stockholm
SWEDEN

Akademisk avhandling som med tillstånd av Stockholms Universitet framlägges till offentlig granskning för avläggande av Teknologie doktorsexamen i numerisk analys 2009-09-11 i Biblioteket, Sydvästra galleriet, Kungl Tekniska högskolan, Osquars backe 25, Stockholm.

© Måns Elenius, augusti 2009

Tryck: Universitetsservice US AB

Abstract

The understanding of complex condensed matter systems is an area of intense study both in physics and chemistry. In this thesis, some properties of simple liquids with strong energetic preference for tetrahedral local ordering has been explored. Tetrahedral order is incompatible with filling the space and hence promotes complex, aperiodic, structures. Consequently, the liquids studied are amenable to supercooling, and give complex crystalline structures on eventual crystallisation. The supercooled liquid state is of interest in its own, showing intriguing anomalies in comparison with the normal liquid state. Understanding supercooled liquids is also a key to understanding glass formation. All liquids studied are simple and monatomic and they are all similar to real metallic liquids. All simulations have been conducted using molecular dynamics. The results presented in this thesis are shortly summarised below.

The complete vibrational density of states of a glass created in simulation has been calculated. The glass was obtained by quenching a liquid. The vibrational density of states for the glass and the corresponding crystalline phase (the σ-phase, a Frank-Kasper crystal) were compared. We show that there is a clear correspondence between the vibrational properties of the crystal and the glass, indicating that the vibrational spectra of crystals can be used to understand the more complex vibrational spectra of the glass of the same substance.

The dynamics of supercooled liquids has been investigated using a previously not implemented comprehensive measure of structural relaxation. We show that this new measure decays more slowly than the commonly used structural relaxation measure (the decay of the intermediate scattering function for the main peak of the structure factor) in the deeply supercooled domain. This indicates that there are relaxation mechanisms in deeply supercooled liquids that are not possible to describe by using a pairwise approximation. This result further strengthen the hypothesis that the structural relaxation of deeply supercooled liquids is a highly collective process.

A new atomic model for octagonal quasicrystals is presented. This model is based on findings from a molecular dynamics simulation of a liquid which crystallised into 45° twinned β-manganese. This twinning of β-manganese is experimentally known to coexist with octagonal quasicrystals. The model quasicrystal is based on an atomic decoration of square and rhombus tiles. The decoration is derived from the β-manganese unit cell and the unit cell of the intermediate structure found at the twinning interface. The advantage over previously proposed atomic models of octagonal quasicrystals is that the side length of the tiles in this model are consistent with experimental results.

Extensive simulations have been used to explore the phase diagram of a liquid at low densities. The resulting phase diagram shows a spinodal line and a phase coexistence region between a liquid and a crystalline phase. The region ends in a critical point, contradicting the old conclusion of the Landau theory of phase transitions – that continuous transitions between liquids and crystals cannot exist.

The phase diagram of the same liquid has also been explored at higher densities. The liquid is known to be fragile at high and intermediate tem-

peratures. Upon cooling the liquid performs a first order liquid-liquid phase transition. The low temperature, high density, liquid is shown to be strong and to have very good glass forming abilities. The structure of the high density liquid is also described in detail. This is the first observation of a first order liquid-liquid transition from a fragile to a strong liquid observed under thermodynamically stable conditions. This result also suggests the possibility of a good metallic glass former.

Contents

Contents **v**

1 Introduction **3**
1.1 Results 4

2 Liquids with tetrahedral local order **5**
2.1 The studied inter atomic potentials 7
2.1.1 The Lennard-Jones potential 8
2.1.2 The IC potential 8
2.1.3 The Z_1 and Z_2 potentials 10
2.1.4 Binary Lennard-Jones mixture 10

3 Molecular dynamics simulations **13**
3.1 Molecular dynamics simulation of simple liquids 13
3.1.1 Periodic boundary conditions 14
3.1.2 Simulation units 16
3.1.3 When is a simulation result relevant? 16
3.2 Measuring structure and structural relaxation 17
3.2.1 Spatial correlation functions 18
3.2.2 Time and frequency dependant correlation functions 19
3.2.3 Structural relaxation in liquids 20

4 Thermodynamics, phases and phase transitions **23**
4.1 Free energy 23
4.2 Phases: crystals, gases and liquids 24
4.3 Phase transitions 25
4.3.1 Spinodal decomposition 26
4.3.2 Critical point 28
4.4 Summary of article 4 28

5 Supercooled liquids and the glassy state: anomalies, theories and landscapes **31**

5.1 Anomalies in supercooled liquids 31
5.1.1 Breaking of the Stokes-Einstein relation 32
5.1.2 Super Arrhenius behaviour 32
5.1.3 Structural and dynamical heterogeneity 33
5.1.4 Non exponential relaxation behaviour 35
5.2 A short overview of the current theories of the supercooled liquid state 36
5.2.1 Cooperatively rearranging regions 36
5.2.2 Mode coupling theory 37
5.2.3 Avoided critical point scenario 37
5.2.4 Ideal glass transition and random first order theory 37
5.3 The glassy state and the glass transition 37
5.3.1 Dynamical properties of glasses 38
5.4 Energy landscapes: a paradigm for understanding the behaviour of the supercooled liquid state 39
5.4.1 Understanding the anomalies of supercooled liquids in terms of the PEL 42
5.5 Summary of article 1 43
5.6 Summary of article 2 44
5.7 Summary of article 5 44

6 Quasicrystals and their structure **45**
6.1 Crystalline symmetry 45
6.2 Quasiperiodicity 47
6.3 A quasiperiodic octagonal tiling and approximants 48
6.4 Atomic structure of quasicrystals 50
6.5 Structure of octagonal quasicrystals 50
6.6 Summary of article 3 52

7 Epistemology of computer simulations in natural science **55**
7.1 Background 55
7.2 How is a simulation created? 56
7.3 An alternative epistemology of simulations 57
7.3.1 Relevance for this thesis 57

Bibliography **59**

Acknowledgements

First I would like to thank my supervisor Mikhail Dzugutov. Both for his sincere interest in, and guidance throughout, the studies leading to this thesis, and for many, often heated, discussions. He has showed me the ways and focus of a person dedicated to science. I would also like to thank Tomas Oppelstrup and Erik von Schwerin who have both offered great company and helped me with practical as well as scientific problems. The collaboration with Daniel Fredrickson and Sven Lidin widened my academic perspective and also provided opportunities for nice coffee breaks and lunches. The staff at PDC has always been helpful and have provided the means for the massive calculations this thesis is based on. Both the PDC-staff and the numerics group at CSC have been been available for necessities such as lunch company and discussions of everything and nothing. I would also like to thank my wonderful family for support and especially my wife Gitte Ekdahl and my father Kjell Elenius who have read and commented the complete thesis before print.

Chapter 1

Introduction

Glasses have been used by humans for several milennia. The material has been of practical use for containers and windows as well as a material for artwork. Visiting a glass works and seeing the glowing molten glass formed into beautiful objects gives an almost magic feel to the material. The long use and general availability of glasses manifests in a popular understanding of the material. As written by Angell [3]:

"Glass, in the popular and basically correct conception, is a liquid that has lost its ability to flow. Thus instead of 'taking the shape of its container,' it can itself serve as a container of liquids."

However, science is not satisfied with descriptions that are "basically correct", and the study of glass and glass formation is a lively field. A quote by Nobel laureate P. W. Anderson [68]:

"The deepest and most interesting unsolved problem in solid state theory is probably the theory of the nature of glass and the glass transition"

signifies the great interest and importance of increasing our understanding of these phenomena.

The glass most commonly known today as well as historically is silica – the material of windows and drinking glasses. The glasses and glass forming liquids discussed in this thesis are most close to metallic glasses, a far more recent discovery. The reason for the discrepancy in time of discovery is that, while silica forms a glass when cooled at rates of about 10^{-2} Kelvin per second, most metallic glasses must be cooled at rates exceeding 10^{5} Kelvin per second to avoid crystallisation. This makes them hard to create in the first place and very hard to create in other forms than very thin objects to allow such rapid cooling. Regardless of the differences between metallic and classic glass formers it is generally believed that the glass

transition is the same phenomenon in both cases. Hence, the study of metallic glasses contributes to our general knowledge of glass formation in general.

Though not as ubiquitous as windows, metallic glasses have their place in our everyday life. The uses of metallic glasses include read heads in magnetic storage devices, coatings in tough and corrosive environments and golf clubs. In practise metallic glasses are created in a cookbook fashion, trying to find a mix of atoms that have no simple crystalline structure. In this way it has been possible to construct metallic glasses that are almost as good glass formers as the classic ones, thus making it possible to create bulk structures of metallic glasses. For the reader interested in technological applications and industrial production of metallic glasses Lindsay Greer has written an easily read introduction [39].

Quasicrystals represent another, more recent, discovery in the world of solid state physics. Originally reported in 1984 they spurred a huge amount of activity and also controversy. Although the controversy has died, the activity is still high. Being a recent contribution to our catalogue of possible states of matter quasicrystals, contrary to glasses, are more or less publicly unknown and so far have limited use in everyday life (even though it is possible to buy cookware coated with quasicrystals). Basic research is still needed to understand fundamental properties and to determine possible uses of these materials.

The common feature for the work presented in this thesis is molecular dynamics simulation of liquids with tetrahedral local order. Why it is interesting to specifically study tetrahedrally ordered liquids is discussed in Chapter 2. The molecular dynamics simulations and some fundamental data analysis is presented in Chapter 3. In the concluding chapter we will touch the subject of the epistemology of physics simulations in general.

1.1 Results

In this thesis a collection of articles is presented in context. Glass and supercooled liquids, together with results on the vibrational properties of glasses (Article 1), the dynamics in supercooled liquids (Article 2) and a thermodynamically stable fragile to strong polyamorphous transition in a simple monatomic liquid (Article 5) are presented in Chapter 5. Quasicrystals in general and the structure of octagonal quasicrystals (Article 3) are presented in Chapter 6. Chapter 4 contains a short presentation of thermodynamics, phases of matter and results on phase coexistence and a critical point between a liquid and a crystal in a simple system (Article 4). In each of these chapters the introductory text gives an overview of the field with focus on the facts necessary to put the result of the corresponding article(s) in perspective. Considering the vastness of these subjects and the restricted size of this thesis the overview will often be painfully short and also incomplete in parts. In an effort to amend this – a large number of references for further reading is given.

Chapter 2

Liquids with tetrahedral local order

The local atomic configuration is a fundamental property of a material. The whole field of crystallography is concerned with finding this property for crystalline solids. The fact that our understanding of liquids and glasses is less developed than that of crystals is related to their lack of a simple, space filling and repeated local atomic configuration. At the same time they are so dense that local atomic structure control their behaviour. In gases we arrive at the extreme where the local atomic configuration can be assumed to be completely random, a situation more easily understood than the intermediate case of liquids and glasses.

It turns out that tetrahedral and icosahedral packings are essential in many interesting materials, e.g. complex crystals such as the Frank-Kasper phases [29] and the β-Mn discussed in Article 3. They are also fundamental in quasicrystals [48, 49], which we will discuss in more depth in Chapter 6. Icosahedra were hypothesised to be fundamental in maintaining liquids in a supercooled state already in the middle of the previous century [28]. A large number of icosahedra and polytetrahedral clusters has also been found in the inherent structures (see Section 5.4) of simulated supercooled liquids, e.g. in Lennard-Jones [80] and in the liquids studied in this thesis [93]. For the network forming liquids that have been intensely studied by e.g. Angell [4] the formation of tetrahedral networks is fundamental. Figure 2.1 gives an example of a tetrahedral cluster created in a simulation of the Z_2 liquid described in Section 2.1.3.

The reason for all this interesting behaviour is the inherent frustration in a tetrahedrally close packed structure. In a dense system strict tetrahedral packing is impossible, simply because there is no way to fill the space with regular tetrahedra without holes. This is similar to the fact that it is impossible to fill the space without holes using spheres, while it is simple using cubes. In figure 2.2 five regular tetrahedra are placed next to each other and the resulting gap can be seen (the gap corresponds to about a tenth of the tetrahedral edge). With minor distortion regular tetrahedra can be packed into regular icosahedra, but regular icosahedra are also impossible to pack in a way that fills the space without holes. A very

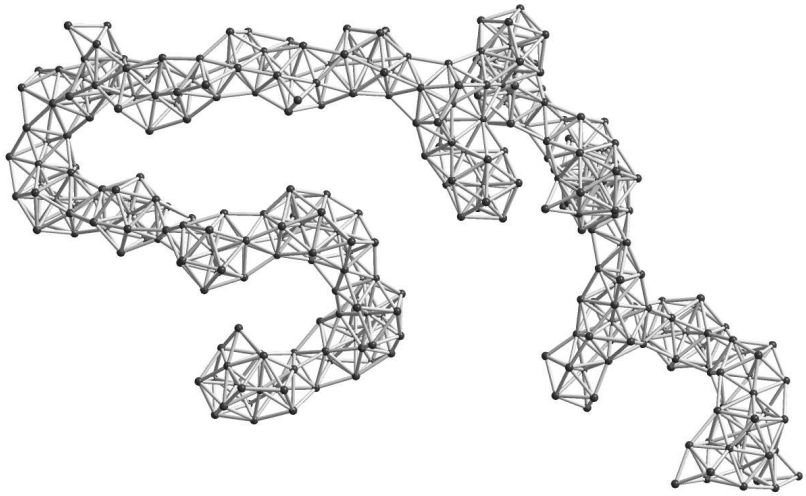

Figure 2.1: An example of a polytetrahedral cluster formed in a simulation of the Z_2 liquid at temperature 0.32 and number density 0.32. This cluster is the largest cluster of face sharing tetrahedra in an inherent structure taken from that simulation. Note that the atoms are plotted with a radius of 10% of the first potential minima to make the structure transparent. Atom pairs with a distance corresponding to the first potential minimum are bonded.

recent discussion of the frustration of icosahedrally ordered systems, particularly Frank-Kasper phases, can be found in reference [67] and a thorough and recent discussion of the matter can be found in reference [86].

It is the atomic interaction that decides the energetically preferred local structure of a material. In dense systems of atoms interacting via a potential that is attractive at medium ranges, e.g. the Lennard-Jones (LJ) potential (see Section 2.1.1), the minimisation of energy boils down to finding the most dense packing, preferably with as many inter atomic distances as possible being that of the minima of the interaction. For four identical atoms it is clear that a regular tetrahedral arrangement with one atom in each vertex is energetically preferred. In this arrangement all atoms have all neighbours at the same distance. The densest competing crystalline ways of packing are the face-centred cubic (fcc), and the hexagonal close packing (hcp) [54] packings. Calculation yields that, using the LJ potential and 13 atoms, the icosahedra has the lowest energy of all these structures, making it the preferred local packing [48]. This result is also true for the potentials used in this thesis.

Upon supercooling a liquid it locally approaches the energetically more favourable local configurations, a fact nicely shown using molecular dynamics simulations and

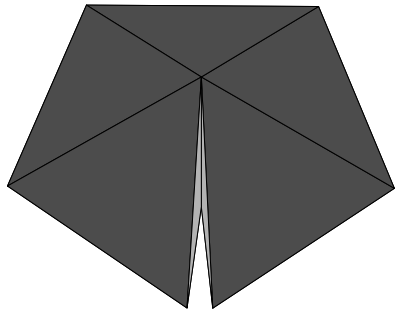

Figure 2.2: Five tetrahedra packed together around a common edge cannot be packed without frustration. The visible gap corresponds to 7.36°.

the potential energy landscapes discussed in Section 5.4 [74]. If a simple crystalline structure exists, then grains of the crystalline structure can form easily when the liquid is supercooled. When a crystalline grain reaches critical size the liquid solidifies into the crystalline structure. Not surprisingly, liquids which easily form crystalline nuclei quickly crystallise on supercooling [3].

The LJ liquid, in which the icosahedral arrangement is preferred locally and which is also known to show an abundance of icosahedral clusters at low temperatures [80], crystallises rather easily to FCC under cooling. The reason for this is that, even though the icosahedral packing is locally preferred, the FCC packing is not much less energetically effective. FCC also has the huge advantage of being able to fill the space without frustration. This lack of simple liquid models able to withstand supercooling without crystallisation, and the great interest in icosahedral liquids [48, 49], spurred the development of the liquids studied in this thesis.

2.1 The studied inter atomic potentials

The potentials used in this thesis are all conjectured to yield interesting qualitative results, not to model any specific real material. On the other hand they are created with the knowledge of effective liquid metal potentials in mind, connecting them to real systems. The reader interested in pair potentials based on real materials is referred to work by Ashcroft [9] and Dzugutov [20, 23].

We have restricted our models to a single atomic species interacting with a pairwise interaction force. There are several advantages of using a single component

liquid with only pair interactions in simulations. The simulation is computationally fast since the force calculation loop is simplified. More importantly, the interpretation of the results is more straightforward since there is no need to discriminate between different atomic species. Hence it is arguable that performing simulations on single component systems is preferable whenever possible.

Metallic liquids seem to be well described using this kind of simple model as can be seen in the references above. In addition work by Moriarty can be mentioned [66]. He has studied models of molybdenum and shown that, for this system, the many body effects that result in an angular dependence of the interactions are very important to correctly simulate the crystalline solid. In the same study he shows that the same many body effects give negligible contribution to the simulation results for liquid molybdenum.

Now we come to the description of the actual liquids simulated in this thesis. They were all designed by Mikhail Dzugutov's research group before the work with this thesis started. For completeness we will also take a look at the Lennard-Jones liquid and the binary mixture Lennard-Jones liquid. All the interaction potentials discussed in this section are shown in figure 2.3.

2.1.1 The Lennard-Jones potential

One of the most commonly used inter atomic potentials is the Lennard-Jones potential. It was proposed in 1931 by John Lennard-Jones to simulate attractive van der Waals interactions at long ranges together with a strong short range repulsion, mimicking the repulsion between atoms when their electron orbitals overlap. The Lennard-Jones potential is defined as:

$$u(r) = 4\epsilon \left[\left(\frac{r}{\sigma}\right)^{-a} - \left(\frac{r}{\sigma}\right)^{-b} \right] \tag{2.1}$$

where a and b are usually chosen to be 12 and 6 respectively. σ defines the size of the atoms and ϵ defines the depth of the potential. The Lennard-Jones liquid works reasonably well for simulating noble gases; which is not surprising since they mainly interact via van der Waals forces and short range repulsion. In practical simulation the potential is almost always truncated at a cut off distance to speed up calculations.

2.1.2 The IC potential

The interest in supercooled liquids and polytetrahedral arrangements inspired the creation of the potentials used in this thesis. They are all created to favour icosahedral ordering and hence make crystallisation complicated due to geometric frustration. The potentials are similar to the Lennard-Jones potential for short range repulsion. For longer ranges, the inter atomic interaction is tailored to strongly favour tetrahedral and consequently icosahedral packing by making square atomic

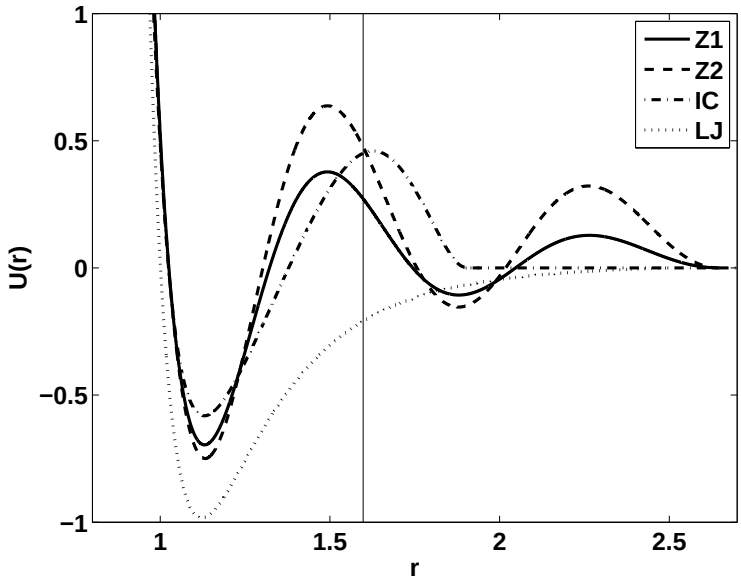

Figure 2.3: The interaction potentials discussed. The vertical line indicates $\sqrt{2}$ times the distance of the first potential minima. For all three potentials used in this work this distance is close to a local energy maximum – inhibiting square packing of atoms.

arrangements energetically punished. This makes it hard for the resulting liquids to find simple packings.

The first potential created with these considerations in mind is known as the (icosahedral) IC-potential [21] having the form:

$$u(r) = A(r^{-p} - B)\exp\left(\frac{c}{r-a}\right)\theta(a-r) + B\exp\left(\frac{d}{r-b}\right)\theta(b-r) \qquad (2.2)$$
$$A = 5.82,\ B = 1.28,\ a = 1.87,\ b = 1.94,\ c = 1.1,\ d = 0.27,\ p = 16\ ,$$

where $\theta(x)$ is the Heaviside function being 0 if x is less than 0 and 1 otherwise. This potential is similar to Lennard-Jones for short distances. On intermediate distances the potential shows a maximum. This maximum is situated at approximately $\sqrt{2}$ times the position of the potential minima, corresponding to the diagonal distance in a square. Hence the maximum discourages square arrangements of atoms. This potential is sometimes referred to as the Dzugutov potential in the literature.

The IC-potential is most widely known for forming a dodecagonal quasicrystal [22]. It generates a moderately fragile liquid with a pronounced tendency for for-

mation of large icosahedrally ordered clusters [93]. In the supercooled state this liquid demonstrates breaking of the Stokes-Einstein relation (see Section 5.1.1). The supercooled liquid also shows dynamical heterogeneities [24].

2.1.3 The Z_1 and Z_2 potentials

Later, two other potentials, Z_1 and Z_2, were designed. They are closely related and share the same functional form with different parameter sets:

$$\begin{aligned} u(r) &= a\frac{e^{\alpha r}}{r^3}\cos(2k_F r) + b\left(\frac{\sigma}{r}\right)^n + V_0 \\ Z_1 &: \ a = 1.58,\ \alpha = -0.22,\ k_F = 4.120,\ b = 4.2\times 10^6,\ \sigma = 0.331, \\ &\quad n = 18,\ r_c = 2.64909,\ V_0 = 0.04682632 \\ Z_2 &: \ a = 1.04,\ \alpha = 0.33,\ k_F = 4.139,\ b = 4.2\times 10^7,\ \sigma = 0.348, \\ &\quad n = 14.5,\ r_c = 2.64488,\ V_0 = 0.13391543 \end{aligned} \tag{2.3}$$

The functional form of these potentials is inspired by the fact that the theory for effective inter atomic interaction in metals yields an oscillating part, an effect that is also found in experiment. These oscillations are called Friedel oscillations and have the functional form:

$$\phi(r) \sim r^{-3}\cos(2k_F r) \tag{2.4}$$

where k_F is the Fermi wave vector [10, 31]. As can be seen the oscillations in equation 2.3 are modelled after this form. k_F is decided by the electronic valency of the material, a property that can be changed by alloying different metals. The parameters in equation 2.3 yield a valency between 2 and 3, values that should be replicable in real alloys.

The oscillatory part and the longer cut of distance gives long range behaviour that clearly distinguishes the Z_1 and Z_2 potentials from the IC potential. The former two have two local maxima and a second local minima.

The Z_1 and Z_2 liquids have pronounced tendencies for tetrahedral and icosahedral ordering [18]. Figure 2.1 shows a polytetrahedral cluster formed in a simulation of the Z_2 liquid at low density. Both liquids also show dynamical heterogeneities in the supercooled state. Z_1 has also been reported to crystallise into the γ-brass structure [25].

2.1.4 Binary Lennard-Jones mixture

For completeness we should also mention a model usually called binary Lennard-Jones (BLJ) [57]. This liquid has been used extensively in the last two decades for simulating glass forming systems. Several results discussed in this thesis where obtained by using it. As the name suggests BLJ is based on the Lennard-Jones potential which is used for all interactions. It differs in that it has two atomic

species A and B and hence two masses, that are chosen to be the same, and three sets of σ and ϵ:

$$\begin{aligned} \sigma_{AA} &= 1.00,\ \epsilon_{AA} = 1.00 \\ \sigma_{AB} &= 0.80,\ \epsilon_{AB} = 1.50 \\ \sigma_{BB} &= 0.88,\ \epsilon_{BB} = 0.50\,. \end{aligned} \tag{2.5}$$

Usually a mixture of 80% A atoms and 20% B atoms is used. BLJ is an adaption of a set of potentials originally created to mimic the behaviour of the metallic system $Ni_{80}P_{20}$. As mentioned above the main disadvantage of a multiple atomic species simulation is that it is harder to analyse the results than for a simulation with one atomic species.

Chapter 3

Molecular dynamics simulations

In this chapter we will discuss molecular dynamics, the main tool used in this thesis. Focus will be on a qualitative description of the main concepts of molecular dynamics simulations, not going into specific algorithms. The main advantage with simulation as compared to experiment is that in a simulation we always know everything about our system. We can study the individual trajectories of atoms, exact atomic positions and local configurations as well as arbitrarily short timescales (large timescales being a problem, as we will see below). The extreme amount of information is not only a treasure trove but also poses problems. It is genuinely hard to extract knowledge from the movements, positions and energies of thousands of atoms making intelligent data analysis fundamental.

The first data to retrieve from molecular dynamics simulations are the free macroscopically measurable quantities like diffusion, pressure, volume, energy or temperature depending on the thermodynamic ensemble simulated. Fortunately all these are easily calculated in a simulation. We will also introduce the density correlation functions that, together with thermodynamic variables, are fundamental in the interpretation of the simulations and in coupling simulations and experimental results.

In the production of results for this thesis a large number of other data analysis tools have been used. These include tools for local structure determination, calculation of vibrational eigenmodes for a disordered system [26], energy minimisation to find the inherent structures fundamental to the analysis of the potential energy landscapes described in Section 5.4 and many more. These tools will not be discussed further.

3.1 Molecular dynamics simulation of simple liquids

The systems studied in this thesis are liquids. We are interested in the microscopic behaviour of these systems and have chosen to do the simulations on the atomic level. We have not used first principle calculations, but are content with simulating

the system classically using only pair interactions and Newtons law:

$$m_i \ddot{\mathbf{r}}_i = \mathbf{F}_i, \quad i = 1, 2, \ldots, N \,, \tag{3.1}$$

where N is the number of atoms, $\ddot{\mathbf{r}}$ is the second derivative of the atomic positions with respect to time, m are the atomic masses and $\mathbf{F}$ is the force acting on the atoms. There exists a vast literature on the topic of molecular dynamics simulations, see e.g. the references [40, 43], so the discussion here will be very brief. The particular implementation used in this thesis has been described in detail in the doctoral thesis of Sergei Simdyankin [77] which is available on the Internet. In the current work the only changes in the code described there is the introduction of MPI-parallelisation.

The basic algorithm for any molecular dynamics simulation has the form:

- Calculate the force acting on all atoms due to the inter atomic potential.
- Update the atomic positions and velocities based on the forces.
- Repeat.

For time integration the code used here implement the leap-frog Verlet algorithm [43], the explicit formula of which is:

$$\begin{aligned} \mathbf{v}(t + \Delta t/2) &= \mathbf{v}(t - \Delta t/2) + \mathbf{a}(t)\Delta t \\ \mathbf{r}(t + \Delta t) &= \mathbf{r}(t) + \mathbf{v}(t + \Delta t/2)\Delta t \,. \end{aligned} \tag{3.2}$$

This integration scheme yields an error of order Δt^4 for the positions of atoms and Δt^2 for the velocities.

3.1.1 Periodic boundary conditions

A real macroscopic system contains on the level of 10^{23} atoms, a simulation of which is intractable for the foreseeable future. To circumvent this problem periodic boundary conditions are used, as they enable simulation of bulk systems while avoiding that the simulation gets unwieldy. This technique is universally accepted and is used in almost all molecular dynamics simulations where bulk properties of matter are studied. In simulations using periodic boundaries, bulk properties of liquids has been reproduced using only some hundreds of atoms. Caution must be taken with the size of the box related to the interaction distance and the distance on which structural correlations exist in the liquid. If the side of the periodic box is smaller than any of these lengths, the result will inevitably be tainted by artifacts, although not necessarily useless.

Figure 3.1 gives a visualisation of how periodic boundaries work. The effect of the periodic boundaries is that the simulation box is surrounded by identical copies of itself in all directions. For the dynamics this means that when an atom moves over the edge of the simulation box, the image atom in the copied box on the opposite side will enter the simulation box, keeping the number of atoms and

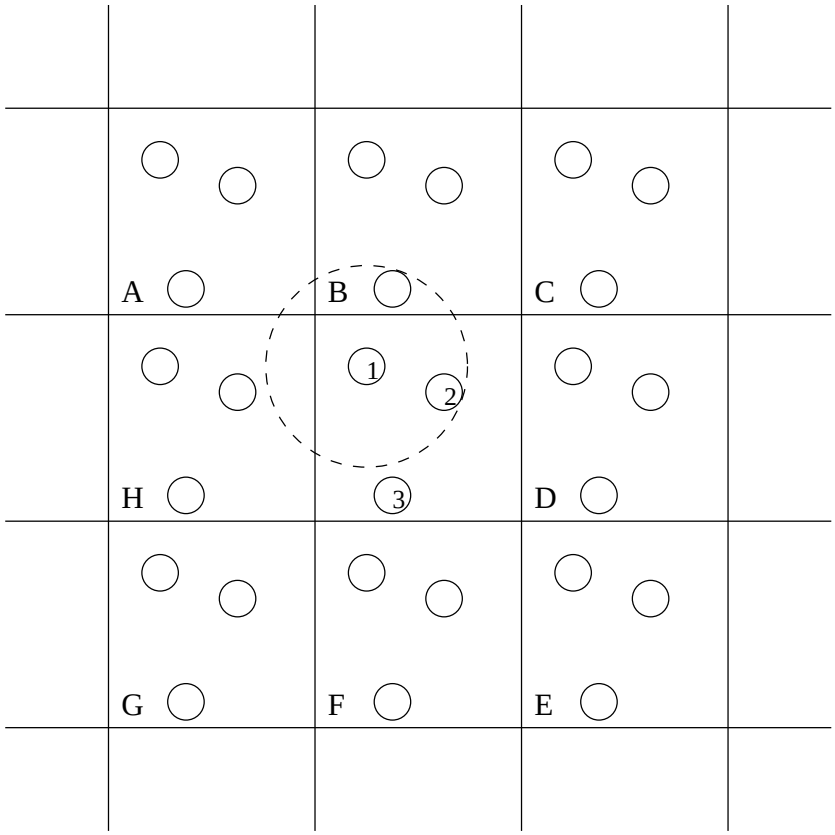

Figure 3.1: A two dimensional system with periodic boundaries. For the argument we assume that the interaction distance is equal to half the box length. The central box is the one where the simulation takes place and the surrounding boxes are copies of the central box. The periodic boundaries gives that, when calculating the interaction between atom 1 and the other atoms in the sample, the interaction will be calculated between atom 1 and the atoms inside the circle. For the atoms named 2 and 3 atom 1 will interact with atom 2 in the central box and with the image of atom 3 in box B. (This plot has been reproduced from [77] with the kind permission of Sergei Simdyankin)

the total momentum in the simulation constant. The interactions are calculated between the atoms in the box and the closest image of all other atoms in the simulation. This is described in more detail in the caption of Figure 3.1.

Another issue solved by introducing periodic boundary conditions is that of surface tension. Real liquids always have surface tension, keeping droplets of the

liquid together. If the surface tension was not there the liquid would not be the thermodynamically stable state and it would immediately evaporate. This effect is not pairwise, but (in the case of liquid metals) depends on the interactions between the positively charged ions of atoms and the negatively charged surrounding electron cloud. When modelling a liquid by using pair forces the electrons, and their cohesive effect, are neglected. The use of periodic boundary conditions restricts the volume of our simulation, not allowing the atoms to change how densely they are packed on the global scale. In this way the periodic boundary conditions keep the liquid dense without the need to include a cohesive force mimicking the effect of surface tension.

3.1.2 Simulation units

When performing computer simulations it is reasonable, both for numerical reasons and convenience, to rescale all physical quantities to numbers of order one. All simulation data presented in this thesis are in such reduced units. The reduced units correspond to those of the Lennard-Jones potential described in Section 2.1. In practise this means that the length unit is defined as the onset of hard repulsion[1]. The mass unit is the mass of a single atom. The energy unit is equal to the depth of the first minimum of the potential and the time unit is derived from the other three. For the other potentials it is still the potential depth of the Lennard-Jones potential that is used as energy unit. All densities are number densities, i.e. the number of atoms per unit volume.

Values for a particular physical system can be retrieved by rescaling. If the parameters of the Lennard-Jones potential are fitted to experimental data for argon the resulting time unit is 2.15×10^{-12} s. Molecular dynamics simulations are usually performed with time steps of at most around 0.01 of the simulation time unit. To simulate a full second then requires approximately 5×10^{13} time steps. As a comparison the longest simulations performed in the work presented here are just short of 10^{10} time steps using 3456 atoms. Performing these simulations required around ten thousand hours of computer (core) time.

3.1.3 When is a simulation result relevant?

It should be noted that the goal of molecular dynamics simulations is never to exactly calculate the atom trajectories. Doing that would simply be impossible while using finite precision (and using infinite precision is not an option). Instead we are interested in getting a relevant sampling of the phase space of the system corresponding to a certain statistical mechanical ensemble. In our case the system is simulated with constant number of atoms and either constant energy and volume (microcanonical ensemble) or constant temperature and volume (canonical ensemble). Thermodynamic quantities are then calculated as averages over a long series of time steps.

[1] The first crossing of the potential function and the x-axis.

Calculating thermodynamic quantities is only relevant for a system that is in ergodic equilibrium. Ergodicity implies that the complete phase space[2] of a system is sampled according to the current ensemble. In statistical mechanics the fundamental assumption is that, in the ergodic state, time averages where time goes to infinity and ensemble averages where the number atoms goes to infinity are equivalent. Hence, if the system is ergodic we can chose whether to simulate a small system for a long time or a large system for a short time to get the same accuracy for our thermodynamic variables.

For supercooled liquids this simple definition breaks immediately since the complete phase space also includes the crystal which is known to be thermodynamically more stable. To avoid this we look at ergodicity for a limited region of phase space (called a phase space component), e.g. the component corresponding to the supercooled liquid in metastable equilibrium. The idea of dividing the phase space into components was discussed by Palmer in the beginning of the eighties [69].

To test ergodicity in a simulation of liquid phases we use the following two criteria:

1. The averages of the free thermodynamic variables have converged.

2. The structure of the liquid measured using $F(Q_m, t)$ relaxes as described in Section 3.2.3.

The first criterion ensures that no phase transitions or other relaxation phenomena are ongoing. The second criterion ensures that we really have a liquid and that our simulation timescale is large enough to resolve the relaxational behaviour of the liquid.

When simulating a crystallisation as in Article 4, criteria number 2 above will not be fulfilled since the structure of a crystal does not relax over time. Still the crystal itself can be seen as one of the phase space components of Palmer. In the crystalline case averaging over a long run is not enough though, since a crystal created by freezing from a liquid will contain a different set of defects for different starting conditions. To achieve a sound statistical ground for the measured values it may be necessary to perform several freezings from different initial liquid states and average over these.

Further discussion of the epistemology of simulations in general can be found in Chapter 7.

3.2 Measuring structure and structural relaxation

In this section we will introduce the pairwise correlation functions most commonly used in the analysis of liquids. Some of them are directly accessible experimentally and simulations allow direct calculation of all of them. They are interrelated by

[2]The phase space is the 6N dimensional space of all atomic positions and velocities. The configurational part of the phase space is discussed in detail in Section 5.4.

Fourier transforms. A complete discussion of these correlation quantities can be found in reference [41].

It is possible to define and use higher order correlation functions. They describe correlations between more than two atomic positions. Such correlation functions are also used in the study of supercooled liquids, see e.g. reference [35]. However, no such correlation functions have been used in the work presented here, and they are not described in this thesis.

3.2.1 Spatial correlation functions

In simulations the most intuitive and easily calculated structural quantity for a simple liquid is the radial distribution function $g(\mathbf{r})$ defined as:

$$g(\mathbf{r}) = \frac{1}{\rho} \left\langle \frac{1}{N} \sum_{i=1,\, j=1,\, j\neq i}^{N} \sum^{N} \delta(\mathbf{r} + \mathbf{r}_j - \mathbf{r}_i) \right\rangle \tag{3.3}$$

where $\delta(\mathbf{x})$ is the Dirac delta function, and ρ is the number density. The division by ρ normalises the value of $g(\mathbf{r})$ to 1 in the long distance limit. The product $\rho \cdot g(\mathbf{r})$ corresponds to the probability distribution of, given a reference atom, finding a neighbour at position $\mathbf{r}$. In isotropic systems like liquids or glasses the direction of $\mathbf{r}$ does not matter and the function is almost always written using $r = |\mathbf{r}|$ as $g(r)$ – the neighbour distribution related only to distance. This is true for all correlation functions discussed here, but we will keep the vector notation for generality. An example of $g(r)$ calculated from a simulation can be found in figure 3.2.

One central feature of liquids is the limited range of pair correlations. The function usually attains its limit value of 1 well before r reaches 10 atomic diameters. Also for more exotic cases, where the spatial correlation extends further, there is a clear qualitative difference between the behaviour of liquids or glasses, and ordered phases such as crystals where the spatial correlation, in principle, extends to infinity.

In experiments the radial distribution function is impossible to measure directly. Fortunately the Fourier transform of $g(\mathbf{r})$ gives a function called the static structure factor:

$$S(\mathbf{Q}) = 1 + \rho \int_0^\infty \exp\left[-i\mathbf{Q} \cdot \mathbf{r}\right] g(\mathbf{r})\, d\mathbf{r} \tag{3.4}$$

The leading 1 comes from the δ function that should be present in $g(r = 0)$ but which is removed in equation 3.3 by restricting the summation to distinct atoms. This function is readily calculated in diffraction experiments, in fact it is the main tool of crystallography, as is discussed in Section 6.1. An example of $S(Q)$ calculated from a simulation can be found in figure 3.3. From experimental results $g(\mathbf{r})$ can be calculated as the inverse Fourier transform of $S(\mathbf{Q})$.

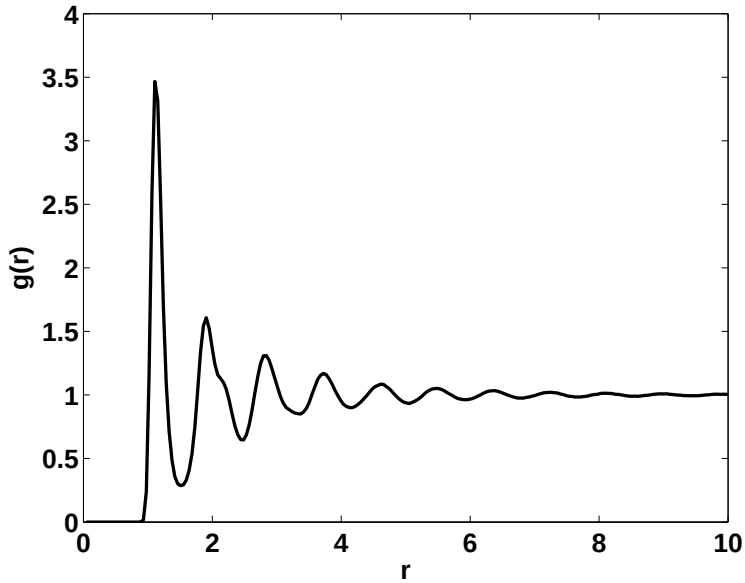

Figure 3.2: $g(r)$ calculated for the Z_2 liquid at density 0.85 and temperature 0.80. At this density and temperature the liquid is in a supercooled state. The Z_2 liquid has a long correlation length since $g(r)$ decays just before $r = 10$.

3.2.2 Time and frequency dependant correlation functions

It is possible to define a time dependent version of $g(\mathbf{r})$ as:

$$g(\mathbf{r}, t) = \frac{1}{\rho} \left\langle \frac{1}{N} \sum_{i=1}^{N} \sum_{j=1}^{N} \delta \left[\mathbf{r} + \mathbf{r}_j(0) - \mathbf{r}_i(t) \right] \right\rangle \tag{3.5}$$

$g(\mathbf{r}, t)$ relates the density in position $\mathbf{r}$ at time t, given that there was an atom at $\mathbf{r} = 0$ at time 0. Obviously, for $t = 0$ we have $g(\mathbf{r}, 0) = g(\mathbf{r}) + \delta(0)$, the δ function coming from the fact that the summation in $g(\mathbf{r}, 0)$ is not restricted to distinct atoms.

Fourier transformation of $\mathbf{r}$ can be carried out for $g(\mathbf{r}, t)$ in the same way as for $g(\mathbf{r})$ to yield:

$$F(\mathbf{Q}, t) = \rho \int_0^\infty \exp\left[-i\mathbf{Q} \cdot \mathbf{r}\right] g(\mathbf{r}, t)\, d\mathbf{r} \tag{3.6}$$

a quantity called the intermediate scattering function[3]. The intermediate scattering

[3]The use of $F(\mathbf{Q}, t)$ instead of $S(\mathbf{Q}, t)$ for this quantity comes from historical reasons not

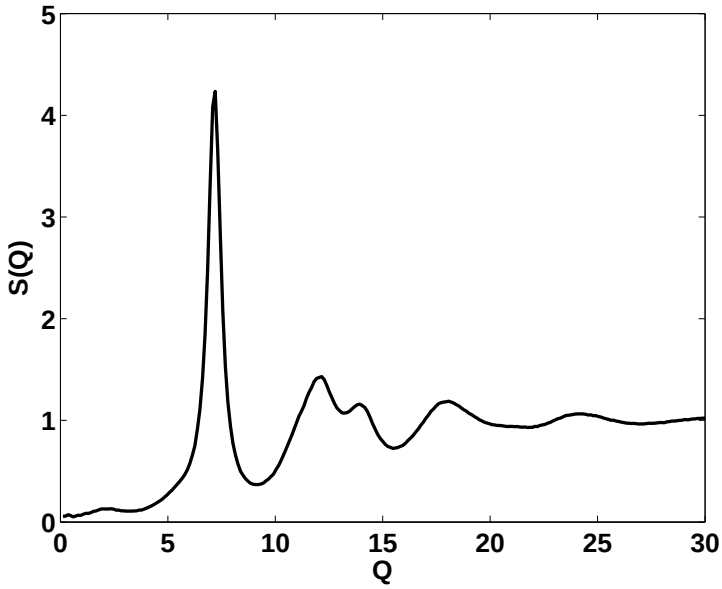

Figure 3.3: $S(Q)$ retrieved by Fourier transform of the $g(r)$ shown in figure 3.2. To the untrained eye this may not say much, but for an expert some conclusions are possible to draw from this figure. These include that the liquid is uniform (since the limit for small Q is 0) and that it seems to have icosahedral local order (the split of the second peak of $S(Q)$ is a signature of icosahedral ordering).

function measures the density correlations between the system at times 0 and t for the wavelength $\mathbf{Q}$.

The intermediate scattering function is not immediately accessible by experiments, but it is possible to measure the spectrum of $F(\mathbf{Q}, t)$:

$$S(\mathbf{Q}, \omega) = \frac{1}{2\pi} \int_{-\infty}^{\infty} \exp\left[-i\omega t\right] F(\mathbf{Q}, t)\, dt \tag{3.7}$$

the integral of which, over all ω, returns us back to $S(\mathbf{Q})$. Hence we have closed the circle of relationships between the different pairwise correlation functions.

3.2.3 Structural relaxation in liquids

The fact that the radial distribution function $g(r)$ decays to 1 beyond a finite distance r_{corr} is a fundamental property of the liquid state. It implies that atomic

known by the author of this thesis.

positions in liquids separated by a distance larger than r_{corr} are not correlated. This in turn implies that structural relaxation in liquids is a purely local phenomenon.

Structural relaxation of liquids is measured by studying the decay of the intermediate scattering function $F(Q,t)$ for the most slowly decaying Q. $F(Q,t)$ is described in Section 3.2.1 with Q as a vector, but for isotropic systems the direction is irrelevant so here we use only the magnitude. Intuitively it is obvious that heterogeneities takes longer to relax if the scale of the heterogeneity is larger, corresponding to smaller Q. This is quantified by the fact that the relaxation time for a specific Q is proportional to $S(Q)/Q^2$ [41]. For ordinary liquids it turns out that the main peak, which occurs for $Q \approx 7$ in reduced units, is slowest and hence dominates the relaxation. In more exotic cases like the low density liquid of Article 4 there can be other peaks that dominate the relaxation.

Chapter 4

Thermodynamics, phases and phase transitions

Thermodynamics is concerned with the behaviour of matter in a physical environment. Both the environment and the matter itself are described by using thermodynamic variables as pressure (P), volume (V), temperature (T), entropy (S), potential energy (U) and total energy (E). Other variables are possible, like the number of atoms and the chemical potential or the electrical charge and the surrounding electric field, but the ones above will suffice for our purposes. The variables can be either extensive or intensive. Extensive variables are proportional to the system size (V, S, U and E) and intensive variables are independent of the system size (T and P).

A full thermodynamic description of a material connects the thermodynamic variables by equations of state. Analytically finding the equations of state is impossible for complicated systems and consequently we study the relations of the thermodynamic variables in experiments and simulations.

4.1 Free energy

The thermodynamic state of a substance at specific conditions can be decided by minimisation of the relevant thermodynamic potential. Which thermodynamic potential to use depends on which variables are free and which are fixed for the system. The word ensemble is used to define the environment of the substance, often together with three letters specifying which thermodynamic variables are fixed. In the NVE (or microcanonical) ensemble the Helmholtz free energy $F = U - TS$ is minimised, in the NVT (or canonical) ensemble the enthalpy $H = U + PV$ is minimised and in the NPT (or isobaric canonical) ensemble the Gibbs free energy $G = U + PV - TS$ is minimised. In the following we will discuss the behaviour of thermodynamic systems using the Gibbs free energy.

Minimisation of the Gibbs free energy $G = U + PV - TS$ in the NPT ensemble

implies that the system strives to minimise its potential energy (U), minimise the used volume (V) while trying to maximise its entropy (S). The entropy can crudely be identified with the disorder of the system. Increasing the pressure makes minimising the volume more important and increasing the temperature makes maximising disorder more important. As we will see in the next section this has fundamental implications for the behaviour of matter upon changes of its physical environment.

4.2 Phases: crystals, gases and liquids

Everyone is familiar with the fact that matter exists in different phases. Which phase a material takes depends on the physical environment. When reducing the temperature T water freezes to ice while an increase of the temperature leads to vaporisation (boiling). The pressure P determines at which temperatures these transitions occur, e.g. water boils well before reaching 100°C at high altitudes where the pressure is lower. These phase transformations occur between solid, liquid and gas phases of the same material, whereas in chemical transformations the molecular composition of the material itself is changing.

The value of the thermodynamic potential G in the space spanned by the fixed thermodynamic variables P and T defines a surface (for a fixed value of N). The value of G is different for different phases and the phase transitions correspond to places in the P-T-plane where there is a crossover between the Gibbs free energy of e.g. the liquid and the gas. As discussed above the system strives to minimise its free energy. From this point of view we can understand the boiling of water at $T = 100°\mathrm{C}$ at ambient pressure as this being a point in the P-T-plane where G_{water} becomes larger than G_{vapour}.

We can use this understanding to get a crude idea of how the three common states of matter – crystal, liquid and gas – are related. In a crystal the local configuration is well defined and repeats indefinitely, minimising the energy U and the entropy S. Obviously this state is favoured by low temperature. The gas is at the other extreme where the material is completely disordered, maximising S. A situation clearly favoured by high temperature.

In this description a liquid is the intermediate where there is an interplay between all three terms of G, giving a dense but disordered structure. In a liquid there still is a local environment that is on average common to all atoms in the liquid and specific to the particular liquid. This local environment is measured by the radial distribution function $g(r)$ described in Section 3.2.1. This intermediate state is more complicated to describe than the crystal and gas states because there is no simple extrapolation to an ideal model (the perfect crystal and the ideal gas for crystals and gases respectively).

A liquid is defined by the fact that it is thermodynamically isotropic (i.e. isotropic on long enough timescales) and that it does not retain any of its structure over time. Simple liquids are isotropic everywhere always, i.e. on all timescales and lenghtscales. There exists comprehensive literature on the properties of simple

liquids in the normal state, the reader is referred to the book by Hansen and McDonald [41] or the old review by Barker and Henderson [11]. In supercooled liquids some of the relations true for normal liquids are broken as discussed in Section 5.1. The solidified amorphous state, the glass, is treated in Section 5.3.

4.3 Phase transitions

Phase transitions can be divided into different categories. In first order phase transitions the substance stepwise transforms from one structure to another, as in the transitions discussed in Section 4.2. This process includes consuming or releasing energy, the amount of which is called the latent heat of the transition. These transitions are accompanied by a discontinuity in the thermodynamical state variables. Examples from everyday life include melting of ice and boiling of water. There is no mistaking the fact that there is a definite difference between vapourised and liquid water, neither that the transformation is discontinuous in parameters such as volume.

The other kind of transitions are continuous, sometimes called second order transitions which is a special case of all continuous transitions. In these transitions the change in structure is not stepwise but occurs continuously. There are no discontinuities in the thermodynamic state variables for continuous transitions, but there are discontinuities in their derivatives of some order[1]. Second order transitions are associated with fluctuations whose length scale diverges close to the transition point. It can at times be hard to discern the order of a continuous transition and it is reasonable to disregard this distinction and categorise them all as continuous [63].

Common to all phase transitions is that it is reasonable and intuitive to describe them by using an order parameter. The order parameter has a step at the transition point for first order transitions while it changes continuously for continuous transitions. Usually the order parameter is defined so that it is zero in one of the phases and non-zero in the other. Landau has constructed a theory of phase transitions based on order parameters [60]. For liquid-crystal transitions the change in global symmetry is usually used as order parameter, while liquid-gas transitions are described using the density as order parameter.

The study of phase transitions is a vast field. In this section we will try to set the context for the results presented in Article 4. For further reading on this subject the books by Landau and Lifshitz [60], Ma [62] and Anisimov [7] can all be recommended.

[1] If the first derivative has a discontinuity the transition is second order, discontinuities in the second derivative corresponds to third order transitions and so on.

4.3.1 Spinodal decomposition

For some first order phase transitions there exists a region in the V-T-plane[2] where no single phase is stable. Such a region is called a spinodal and a system in a spinodal domain inevitably decomposes into two separate coexisting phases. This is most commonly seen for transitions between liquids and gases but has also been seen for liquid-liquid transitions [30].

The thermodynamic relation defining the spinodal region is $\partial P/\partial V < 0$, i.e. the pressure of the system decreases if the volume increases, a clearly unstable situation. A simple model showing this behaviour has been created by van der Waals and can be found in any textbook on thermodynamics. The van der Waals equation is a modification of the ideal gas equation:

$$PV = Nk_BT \tag{4.1}$$

where k_B is Boltzmann's constant [3]. The modification consists of increasing the pressure and decreasing the available volume. This corresponds to introducing a spatial extent of the atoms, which in the ideal gas model are assumed to be point like. The resulting equation has two parameters a and b and the following form:

$$\left(P + a\left(\frac{N}{V}\right)^2\right)(V - Nb) = Nk_BT\,. \tag{4.2}$$

This equation of state catches many fundamental properties of systems with two fluid[4] phases. The phase diagram of the van der Waals equation is shown in figure 4.1.

For two phases to coexist it is necessary that their pressure, temperature and free energy are equal. This leaves entropy, potential energy and density (the inverse volume) as the quantities that may differ. The coexistence region is created by the fact that the two phases have states of the same G for a set of T and P with different densities. For a coexistence to be possible in a limited system it is also necessary that the interface between the two phases is not too energetically costly.

In first order transitions between a simple liquid and its corresponding crystal there have been no observations of spinodal decomposition. The general understanding of this fact rests on two observations. First, the density difference between liquid and solid is generally small, leaving a small region where coexistence would be beneficial. Second, the difference in symmetry between the two phases implies a large interfacial energy, hindering coexistence. The result is the behaviour usually observed for crystallisations. The supercooled liquid shows formation and destruction of small crystalline grains. Their destruction is due to the large interfacial

[2] We use V instead of P since the pressure is constant in these regions and hence it is not a region but a line in the P-T-plane.

[3] When calculating using reduced units Boltzmann's constant is set to 1. We keep it here since the equations are well known in this form

[4] Here fluid denotes both liquids and gases. As we will shortly see defining them as two different phases is not fundamental.

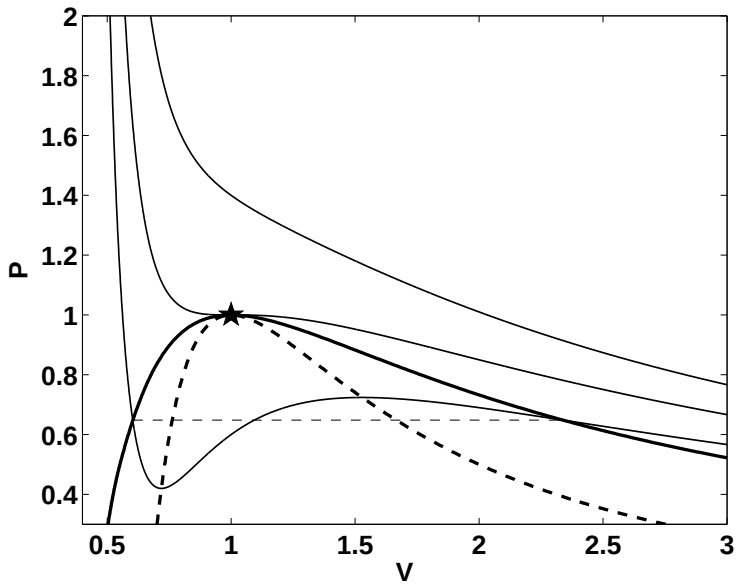

Figure 4.1: The phase diagram of the van der Waals equation (equation 4.2) in the V-P-plane. The thin lines correspond to isotherms. The thick line demarcates the coexistence region and the dashed thick line is the spinodal line within which the isotherms correspond to unstable states. The star marks the critical point. The top isotherm show no irregularities and correspond to $T = 1.1T_c$, the region where there is only one phase. The lowest isotherm correspond to $T = 0.9T_c$ where there are two phases and the isotherm passes the spinodal and coexistence regions. The dashed thin line is the stable thermodynamic value of P for the lowest isotherm in the two phase region. The middle isotherm correspond to $T = T_c$ and shows the flat region expected around the critical point. The variables T, V and P in this figure have all been scaled so that they have the value 1 at the critical point.

energy. Eventually a grain of critical size is formed and then the complete sample crystallises quickly.

4.3.2 Critical point

The coexistence region can end in different ways. In the scenario of interest to us the coexistence and spinodal regions end in a critical point as in figure 4.1. Passing through the critical point the thermodynamic variables of the system have discontinuities similar to the ones seen for second order transitions [7]. The critical point is special since it is the only point on the spinodal line that is thermodynamically stable. At the critical point:

$$\left(\frac{\partial P}{\partial V}\right)_T = \left(\frac{\partial^2 P}{\partial V^2}\right)_T = 0\,. \tag{4.3}$$

The flatness of the pressure with respect to the volume leads to a situation where the fluctuations between the two phases diverge, implying divergence of thermodynamic susceptibilities like the heat capacity.

For temperatures above T_c there is no discernible phase transition. Hence it is possible to move the system between the two phases without any phase transition. In the phase diagram of figure 4.1 any movement from a state to the left of the diagram below T_c to a state to the right of the diagram below T_c not crossing the thick solid line, corresponds to such a transition. The possibility to continuously transform between the liquid and gas phases of a material is what makes the distinction between the two phases questionable.

This has important implications for the existence of a spinodal domain in a first order transition between a simple liquid and its corresponding crystal. If such a spinodal ends in a critical point it would be possible to continuously transform the disordered isotropic liquid into the highly ordered crystal. In fact this scenario is directly discussed and forbidden by Landau in his theory of phase transitions [60]. Later there has been several other authors discussing ways of circumventing the premises of Landau's conclusion, see e.g. reference [13]. In simple systems spinodal decomposition has not been seen between liquid and crystalline phases. However, for some more complex molecules like polymers such spinodals have been observed [33]. In simulations of nano-scale clusters coexistence is seen in time. The cluster may flip between a crystalline and a liquid phase even though they do not physically coexist. The cluster coexistence region in phase space is related to spinodal lines and the first order phase transitions in the respective bulk materials [12, 87].

4.4 Summary of article 4

In Article 4 we report our observations of the phase diagram of the Z_2 liquid at low densities ($0.32 \leq \rho \leq 0.50$). We find that at the higher densities of this interval the system crystallises to a complex crystalline structure on cooling. For intermediate

densities the transition is not directly to the perfect crystal but instead to a spinodal region. The latent heat of the transition is decreasing upon lowering the density until it vanishes for a density of approximately 0.33, a clear indication of a critical point.

Upon cooling the liquid for densities below the critical density we see a continuous transition to a mesophase. The mesophase is still liquid but has an ordering locally similar to that of the crystal. The existence of this mesophase seem important for the existence of the spinodal by reducing the interfacial energy between the liquid and the crystalline phases. The mesophase also offers a way of continuously introducing crystalline order to the originally disordered liquid.

Chapter 5

Supercooled liquids and the glassy state: anomalies, theories and landscapes

When cooling a liquid to a temperature lower than the melting temperature (T_m) of the corresponding solid the liquid is, by definition, in a supercooled state. A large family of liquids crystallise quickly in this state. The liquids we are interested in do not, instead they maintain their liquid status in the metastable, supercooled, state for a range of temperatures below T_m. In this chapter we will look at how relationships and effects in the normal, not supercooled, liquid state break down upon supercooling.

We will also look at the glassy state. A glass is the solid material formed from a liquid under continuous cooling without crystallisation. The temperature where the liquid solidifies is denoted T_G. We will mainly discuss dynamical anomalies in glasses, which is the subject of Article 1. After introducing the anomalies we will make a quick overview of current theories trying to capture the behaviour of supercooled liquids. We will end with a discussion on potential energy landscapes, which have proven to be a very useful for understanding supercooled liquids.

The following discussion of supercooled liquids, glasses and potential energy landscapes is not complete, the interested reader is referred to the short and easily read reviews [3, 17] for an overview or the more recent review [42] for a more thorough discussion. The recent book [86] is recommended, especially for a discussion of liquids and glasses from the perspective of potential energy landscapes. For the ordinary liquid state the reader is referred to the references [11, 41].

5.1 Anomalies in supercooled liquids

This section will give an overview of the differences between normal and supercooled liquids, each subsection discussing a particular effect.

5.1.1 Breaking of the Stokes-Einstein relation

A result for normal liquids, long believed to be generally true for the liquid state, is the Stokes-Einstein relation. It relates the diffusion D and the viscosity η through the temperature T and the (effective) particle diameter r of a liquid:

$$\frac{D\eta}{Tr} = const\,. \tag{5.1}$$

The fact that this relation is broken in deeply supercooled liquids was first noted around the beginning of 1990 [72].

Viscosity is intuitively related to the structural relaxation of a liquid, in fact the two are often used as equivalent, even though this is not really correct. The diffusion (D) is directly coupled to the mean square displacement (msd) of atoms via Fick's law:

$$D = msd/(6t)\,, \quad t \longrightarrow \infty. \tag{5.2}$$

Where t is the time. Hence the Stokes-Einstein relation gives a coupling between the average distance moved by atoms and the structural relaxation for a liquid. The breaking of this relation implies that the atoms on average need to travel farther to achieve structural relaxation. The breaking of the Stokes-Einstein relation seems to occur only for fragile liquids, defined in the next section [17].

5.1.2 Super Arrhenius behaviour

Normal liquids show Arrhenius, exponential, behaviour of the diffusion D with respect to the inverse temperature T^{-1}:

$$D = D_0 \exp\left(-AT^{-1}\right) \tag{5.3}$$

where D_0 and A are constants. Svante Arrhenius originally justified this relation for rates in chemical reactions in the end of the nineteenth century. It has later proven to be a good empirical fit for the diffusion in normal liquids and a large number of other physical properties. This is not surprising since Arrhenius behaviour is expected whenever a property is dependent on an energy barrier.

Upon supercooling the Arrhenius behaviour of diffusion breaks for some liquids. In this region the dependence of the diffusion on temperature is stronger than equation 5.3 suggests. This kind of behaviour is called super Arrhenius. The relationship between D and T after this breaking is often fitted to the equation:

$$D = D_0 \exp \frac{-BT_0}{T - T_0} \quad , \tag{5.4}$$

known as the Vogel-Fultcher-Tamman (VFT) equation. Based on a fit of the viscosity to the VFT equation approaching T_G Angell has proposed a division into strong

and fragile liquids[1] [2]. The larger the deviation from Arrhenius behaviour (corresponding to a smaller value of B) the more fragile is the liquid. Fragility is now accepted as an important characteristic of liquids. The fragility can be calculated for properties such as diffusion, viscosity or any relaxation time. The main plot in figure 5.1 shows how liquids with different fragility behave in an Arrhenius plot of the inverse temperature versus viscosity. There are also other common measures of fragility than B, e.g. the slope of the fitted line in the rightmost part of figure 5.1.

For several liquids a transition between fragile and strong behaviour has been observed. As an example strong liquids tend to become fragile on compression [3] and for a model of silica a fragile to strong transition has been observed on cooling at experimentally inaccessible temperatures [73]. In recent years Angell has argued that all liquids, or at least the family of network forming liquids, have a transition from fragile to strong behaviour upon cooling [4]. In liquids usually described as strong the transition is supposed to have occurred for very high temperatures. For fragile liquids this transition is either hidden by the glass transition or – in the more bold version of this idea – the glass transition is seen as a weak first order transition[2] between the two liquid states [5]. In Article 5 we demonstrate that the Z_2 liquid performs a first order fragile to strong transition where both liquids are thermodynamically stable, a behaviour not previously observed.

5.1.3 Structural and dynamical heterogeneity

In the normal liquid state all behaviour is isotropic in both space and time. This can be seen e.g. in the distribution of the squared atom displacements which is Gaussian, as expected for a random walk. For a supercooled liquid this behaviour breaks and the atomic displacements show a split peak for short timescales, indicating that the liquid is dynamically heterogeneous.

Several investigations, using both molecular dynamics and colloidal suspensions, show that the supercooled liquid is divided into domains for short timescales [24, 58]. Some domains contain fast moving atoms and some contain more slowly moving atoms. Averaged over longer times the individual atomic displacements retain a Gaussian distribution, indicating that on this longer timescale atoms have diffused between the fast and slow domains so that the initial domain of the atom is irrelevant and ergodicity is restored. Note that dynamical ergodicity does not necessarily imply that the sample has structurally relaxed. Diffusion can occur by hopping in and out of the slow domains, making it possible for the atoms to diffuse between different dynamical domains without relaxing the structure of the domains themselves.

[1] It should be noted that the VFT equation does not capture the behaviour over the complete interval where experimental data is accessible [3].

[2] A weak first order transition behaves similarly to second order transitions when the transition point is approached. There is a growth in fluctuations and correlation lengths as well as an increase in e.g. the heat capacity. In difference to a second order transition the complete process is not continuous. Before reaching what would be the criticality in a second order transition there is a discontinuity in the thermodynamic quantities as in a first order transition [27].

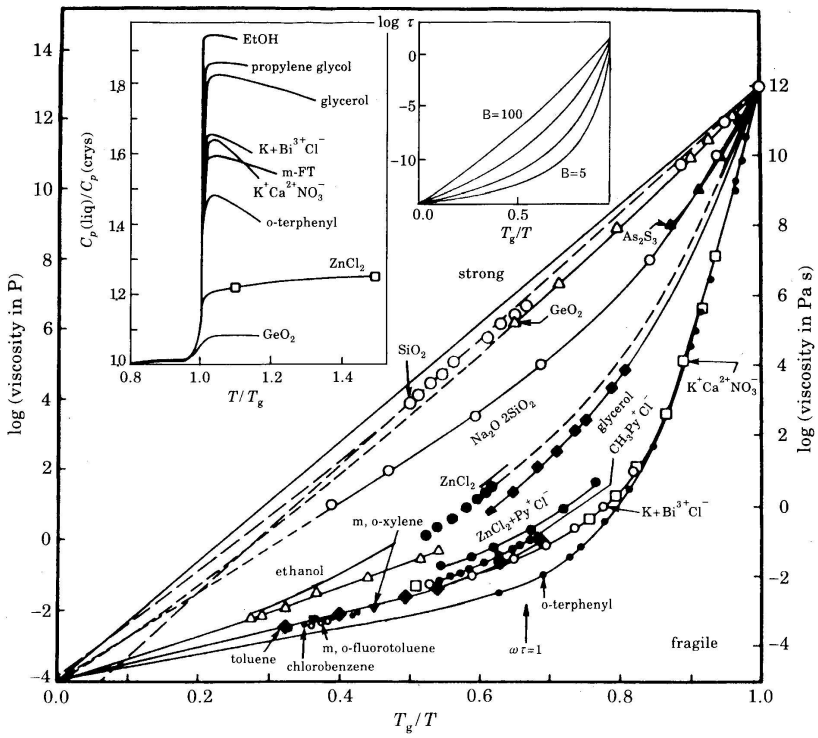

Figure 5.1: The main plot shows a collection of experimental data for different liquid substances. The x-axis is in units of inverse temperature normalised by the glass transition temperature T_G (defined as when the viscosity reaches 10^{12} Pa s). The more curved the approach to the glass transition is, the more fragile is the liquid. The larger insert shows the behaviour of the heat capacity for a supercooled liquid when passing through the glass transition. Here the x-axis is temperature scaled by T_G. As can be seen there is a very sharp drop of the heat capacity at the glass transition. In general more fragile liquids have a larger drop in heat capacity at the glass transition than strong liquids. The small insert shows the behaviour of the Vogel-Fultcher-Tamman equation (equation 5.4) for different values of B, plotted for the same axes as the main plot. (This plot has been adapted from reference [6])

The nature of these domains, and their possible interpretation, often as the cooperatively rearranging regions (CRRs) of Adam and Gibbs (see Section 5.2.1), has attracted a lot of attention. Glotzer et al. are promoting a view where the coherent movement of one dimensional, string like, clusters is the fundamental mechanism responsible for all relaxation [32]. On the other hand Wolynes et al. argue, using the RFOT theory mentioned in Section 5.2.4, that there should be a crossover temperature on cooling where the CRRs change from being one dimensional strings to compact extended regions [82]. Recently Appignanesi et al., using a binary mixture Lennard-Jones liquid (BLJ), showed that the slowest relaxation mechanism takes place as a collective motion in large, compact, clusters involving around 40 atoms [8]. Even more recently de Souza and Wales, also working with BLJ, showed that the super-Arrhenius behaviour of fragile liquids discussed above occurs inside the regions themselves, and not as a result of averaging over the different relaxation times of different exponentially decaying regions [16].

5.1.4 Non exponential relaxation behaviour

In normal liquids relaxation processes are exponential. When supercooling, non exponential relaxation behaviour is noted for both fragile and strong simple liquids [17]. The relaxational behaviour is empirically known to match the following equation called stretch exponential or Kohlrausch-Williams-Watts (KWW):

$$A = A_0 \exp\left[-(t/\tau)^{\beta}\right], \quad (\beta < 1), \tag{5.5}$$

where τ is the relaxation time and β determines the stretching of the relaxation. If β is 1 the relaxation is exponential, if β is smaller than 1 the relaxation is stretched. For the same substance β may vary both between different properties and with temperature. In the mode coupling theory discussed in Section 5.2.2 β is defined by the relaxation process [38].

The relaxation experimentally observed is often stepwise. For short timescales there is a fast relaxation that relaxes the system to a plateau value for the measured quantity. This is followed by a second, often orders of magnitude slower, relaxation process that continues until the measured quantity is completely uncorrelated. The fast relaxation is called β-relaxation and slow relaxation is called α-relaxation. The naming comes from Johari and Goldstein who named the high and low frequency peaks in dielectric loss measurements on liquids β and α respectively [51]. It is the slow α-relaxation that is fitted with the KWW function while the β-relaxation is modelled by Arrhenius behaviour. For temperatures below the glass transition temperature no α-relaxation occurs, i.e. the α-relaxation time is infinite. On the other hand the β-relaxation still persists after the glass transition, still following Arrhenius behaviour [17].

For some liquids there seem to be a correlation between fragility and non-exponential relaxation and there are several publications making this connection [83]. For simple liquids the correlation seem nonexistent, or at least much weaker.

For example strongly non-exponential relaxation behaviour of a model of the generic strong glass former silica has been observed [75, 73].

5.2 A short overview of the current theories of the supercooled liquid state

The effects discussed in Section 5.1 has inspired the development of several different theories all searching to enable an understanding of supercooled liquids and the glass transition. In this section we will very briefly introduce the theories currently active and commonly referred to in the community. The fact that there exist such a diversity of theories indicates both the large interest in, and the limited knowledge of, supercooled liquids.

5.2.1 Cooperatively rearranging regions

One old theoretical model still in wide use is that of Adam and Gibbs [1]. They argue that the liquid can be seen as consisting of regions, called cooperatively rearranging regions (CRR) governing the structural relaxation of the liquid. A CRR is a minimum size region with the possibility to structurally relax without changing its surroundings. They then argue that such a region must have a minimum configurational entropy ($s_{c,CRR} = B_{AG}$) to allow internal movement, and that almost all relaxation will take place in regions with entropy no larger than B_{AG}. The result of the argument is a coupling between the configurational entropy per atom and the structural relaxation. It is often stated as (interchanging relaxation time and diffusion):

$$D = D_0 exp(-B_{AG}/(T s_c(T)) \,. \tag{5.6}$$

This theory has sustained criticism for several reasons. Among them that it is purely phenomenological, and that it assumes that the configurational entropy is spread evenly over the atoms; giving a specific size common to all CRRs – implying a homogeneous liquid. It also turns out that the CRRs seem very small at T_g and that it is possible to construct model potentials with similar s_c but different kinetics [42]. Regardless the criticism the idea of CRRs is still widely used and referred to, especially in relation to heterogeneity in supercooled liquids, see Section 5.1.3. One reason for this is probably that there are numerous examples where equation 5.6 holds [42].

One should be cautioned that different authors use the concept of CRR in slightly different ways. This seems to originate from the theory assuming a homogeneous liquid. Actual supercooled liquids are heterogeneous on short timescales, containing both fast and slow regions. Different researchers seem to map the concept of CRR on different such regions.

5.2.2 Mode coupling theory

Mode coupling theory (MCT) is based on a coupling of the viscosity and the structural relaxation of liquids [37, 34] using functionals acting on the $S(Q,\omega)$ described in Section 3.2.2. The theory originally did not take any heterogeneities of the liquid into account. This original theory is successful in describing the liquid state until the liquid is moderately supercooled. The coupling between structural relaxation and viscosity introduces a singularity upon cooling where the structure freezes. This temperature is denoted T_c and was assumed to correspond to the glass transition temperature T_g in the original MCT.

Now it is known that T_c is significantly larger than T_g. Even so, T_c is still used as a characteristic temperature of a liquid and it might have physical importance as the onset for a new dynamic regime [35, 15]. A probable reason for the failure of the original MCT is the assumption that the supercooled liquid is homogeneous. As discussed above we now know that heterogeneities are important in the description of deeply supercooled liquids. Significant work has been done to remove the singularity at T_c and accommodate experimental results [38, 15], but this is outside the scope of this thesis.

5.2.3 Avoided critical point scenario

Another line of reasoning is the avoided critical point scenario put forward by Kievelson and Tarjus [55, 56]. This scenario assumes that the supercooled liquid has a preferred local structure to which it would like to transform at a temperature significantly above T_G. The transition is inhibited since this preferred local structure is such that it cannot fill the space without frustration. The liquid is left in a "half-transformed" state with fluctuations similar to those around a critical point, see Section 4.3.2.

5.2.4 Ideal glass transition and random first order theory

Kirkpatrick, Thirumalai and Wolynes have put forward another theory, inspired by phase transitions in generalised spin glasses. It divides the supercooled liquid into transient volumes of ideal glass separated by higher energy "membranes" of mobile atoms. The theory has been used to quantitatively calculate stretch exponential relaxation and fragile behaviour. It has a thorough theoretical framework which is outside the scope of this thesis. The interested reader is referred to the references [53, 42] for more information about this theory.

5.3 The glassy state and the glass transition

Amorphous structures or glasses can be formed in a large number of different ways [3, 39]. Here, since the starting point is the simulation of liquids, we focus on glass formation via supercooling a liquid.

When cooling a liquid it eventually solidifies (disregarding helium at low pressures). If it does not crystallise it undergoes what is called a glass transition. The elusiveness of the glass transition is related to the fact that all definitions of it presented so far are subjective. Used definitions include [17]:

- setting a threshold value for the viscosity, usually about 10^{13} Poise
- setting a time limitation on a characteristic molecular relaxation time to e.g. 100 s
- The point where the heat capacity has reached that of the corresponding crystal, as is shown in figure 5.1.

There are clear differences between the glass transition and the thermodynamic first order or continuous transitions (see Chapter 4). In the glass transition the thermodynamic variables changes very rapidly when the system is cooled towards and past T_G, but there are no discontinuities either in the variables or their derivatives. In addition the temperature T_G at which the transition occurs is history dependant. The slower a glass forming liquid is cooled the lower the glass transition temperature using the definitions above. How to understand the glass transition, the similarities and differences when compared to thermodynamic phase transitions, still remains an open question. Currently most researchers in the field seem to agree that the glass transition as observed is a purely kinetic phenomenon [86, 3], though underlying thermodynamic transitions are not ruled out.

5.3.1 Dynamical properties of glasses

The vibrational properties of crystals are well explored and are discussed in fundamental textbooks on solid state physics [10, 54]. The periodicity makes the analysis of the vibrational spectra of perfect crystals relatively simple. It is possible to find a set of orthogonal normal modes in which all possible vibrations can be expressed. Perturbation methods can be used to analyse the phonon spectra for, chemically and or positionally, moderately disordered crystals. In neutron scattering experiments the vibrational properties can be measured through $S(\mathbf{Q}, \omega)$ described in Section 3.2.2.

For a disordered solid the vibrational spectra is more complicated. Complete characteristics of the vibrational spectra of a disordered solid consisting of N atoms requires the calculation of $3N - 3$ vibrational eigenvectors and eigenvalues. The vibrational spectra of a disordered solid differs significantly from that of a perfect crystal – both in the high and low frequency domain. In crystals all vibrational modes are extended in space while for glasses the high frequency modes are strongly localised. This manifests in a cross over frequency for glasses called the the Ioffe-Regel crossover where the mean free path of a vibrational excitation becomes of the order of the inter atomic separation, effectively stopping transmission of high frequencies.

In the low frequency domain there are two observations that stand out when compared to crystalline behaviour. One is seen in the low temperature heat capacity, which is determined by the vibrations of the material around local minima. For crystals the low temperature heat is proportional to the cube of the temperature T^3, while for disordered solids the heat capacity is proportional to T. There is also an excess number of low frequency vibrational modes in amorphous solids, usually referred to as the boson peak. Our understanding of these two effects is not complete, but both have been connected to the existence of two level systems (TLSs). A TLS is a feature of the potential energy landscape discussed in Section 5.4. It correspond to a local transformation between two local potential minima. The transition barrier in a TLS is low and the state before and after transition are (almost) energetically degenerate. A recent and thorough discussion of the dynamic effects of disorder can be found in the recent report by Price, Saboungi and Bermejo [71].

5.4 Energy landscapes: a paradigm for understanding the behaviour of the supercooled liquid state

A viewpoint that has become increasingly popular when studying supercooled liquids, glasses and the glass transition is that of the potential energy landscape (PEL). The idea is that the position of N atoms moving in three dimensions can also be described as a point moving in $3N$ dimensions (assuming the atoms are spherical, more dimensions can be added to describe other degrees of freedom if necessary). For each point in the high dimensional space the potential energy of the system can be calculated and, given that the interaction potential is continuous, will form a continuous surface in $3N + 1$ dimensional space. The recent book by David Wales can be recommended for anyone seeking more knowledge in the area of PELs [86]. The book, in addition to discussing supercooled liquids, handles biomolecules and clusters where the PEL viewpoint is also widely used.

To get some intuition of a PEL and what it implies for the dynamics of supercooled liquids one can start with imagining flying over a real, mountainous, landscape in an airplane. Figure 5.2 gives a very simplified visualisation of a PEL that could also be a topographic map of a mountain range. As long as you fly high enough you are not affected by the mountains and can move freely. This correspond to the normal liquid state in our analogy. Lowering the temperature of the liquid is analogous to reducing the altitude of the airplane. Let us see how the flight of the plane would be affected if it flies randomly and with continuously decreasing altitude (obviously without crashing into the mountains).

First there are some peaks that must be avoided, but essentially the plane is still unaffected by the landscape it flies over. When descending further the effects increase drastically. The number of accessible valleys (analogous to metabasins or inherent structures which are described below) will decrease. Some valleys will simply lie above the current altitude, and reaching other valleys, still lower than the

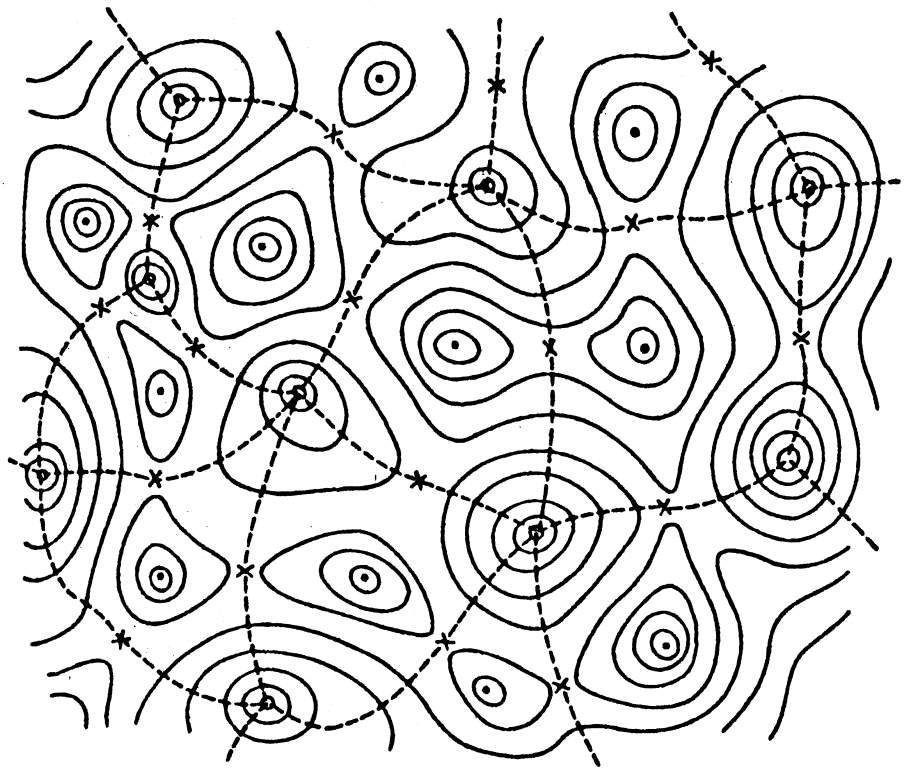

Figure 5.2: A schematic view of an energy landscape in two dimensions. It should be read like a map with contour lines showing the potential energy. The dots are the local minima; commonly denoted inherent structures. The dashed lines are ridges defining the attraction basins of the inherent structures with crosses representing the saddle points (i.e. the lowest possible energy needed to pass between the inherent structures divided by that ridge). This figure has been reproduced from [84] and reprinted with kind permission from AAAS.

current flying altitude, will require passing high passes making them inaccessible. Moving between different valleys would also be much harder, sometimes requiring very long detours compared to the straight line. This situation would correspond to the deeply supercooled, landscape dominated, liquid. Eventually, while continuously decreasing altitude, the plane would get stuck in some valley without any possibility to get out, which would correspond to the liquid-glass transition. The reader should be warned that the geometry of high dimensional spaces defies most, if not all, of our geometric intuition, so this analogy should be used with that in mind.

The PEL approach was first suggested in the end of the sixties in an article by Goldstein where he discusses the concept of the PEL as a surface in $3N+1$ dimensional space [36]. He also qualitatively describes how lowering the temperature of the liquid will lead to a shift from landscape independent to landscape dominated dynamics. In the middle of the eighties, Stillinger and Weber [84], carried the field further with a structured and quantitative analysis of the PEL by molecular dynamics simulations. They used the idea of mapping the configurational trajectory of the system onto the local minima (commonly called inherent structures) of the PEL, which they found by systematically performing energy minimisation on the configurations passed in the simulation. In this way they could divide the liquid properties into a dynamic and a configurational contribution. In the article they made several observations still in common use today, like the fact that the energy of inherent structures in the normal liquid is almost temperature independent. They restricted their study to the normal liquid domain, noting that their conclusions did not seem to hold in the supercooled domain.

The next major step in using energy landscapes to understand supercooled liquids was made by Sastry, Debenedetti and Stillinger [74]. They systematically used the same method as Stillinger and Weber for the BLJ liquid in the supercooled domain for different temperatures and cooling rates. This revealed the pattern shown in figure 5.3.

There are several interesting conclusions to be drawn from figure 5.3. The temperature dependence of the energies of the inherent structures visited by the liquid is markedly different for three different regions. At high temperatures the inherent structure energies are independent of the temperature. Coinciding with the onset of super Arrhenius behaviour (see Section 5.1.2), the inherent structure energies then decrease rapidly with the temperature. Eventually the temperature dependence vanishes again, and the energy saturates on a level dependant on the cooling rate. Slower cooling yields lower saturation energy, apparently since the slower cooling enables the system to explore lower energy minima before it gets stuck. The crossing into the third region is the simulation scale glass transition. The idea that the glass transition corresponds to the trapping of the system in a metastable region of the PEL is strongly corroborated by these observations; so is the notion that supercooled liquids and the glass transition are fundamentally connected to the PEL of the corresponding liquid.

Another example connecting the behaviour of supercooled liquids and their PEL

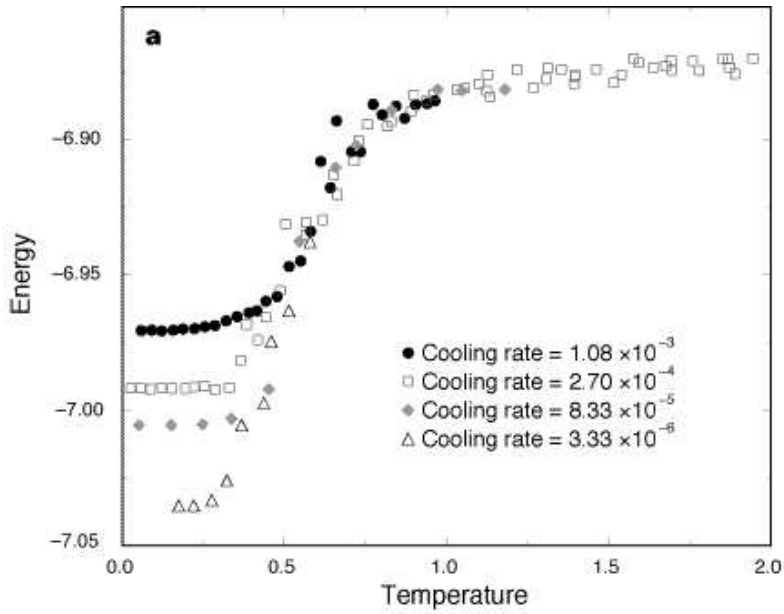

Figure 5.3: This plot shows the inherent structure energies for different temperatures and cooling rates for the binary mixture Lennard-Jones liquid described in Section 2.1. See text for an interpretation of the figure. (This plot has been reproduced from [74] with the kind permission from Nature Publishing Group)

is the transition from fragile to strong behaviour as discussed above. Saika-Voivod et al. has recently made a thorough investigation of liquid silica at different densities [73]. For some densities they see a fragile to strong transition coinciding with an inflection of the inherent structure energy dependence on temperature. For low densities we have seen the same behaviour for our Z_2 liquid, a result not yet published.

5.4.1 Understanding the anomalies of supercooled liquids in terms of the PEL

Heterogeneity and Stokes-Einstein breaking

The short time heterogeneity that seems fundamental to supercooled liquids comes about naturally in the PEL. It has been shown that supercooled liquids show a large spread in barrier heights for transitions between different inherent structures. It is known that such a spread is enough to introduce time limited heterogeneity of the system [86].

The breaking of the Stokes-Einstein relation can be explained by heterogeneous dynamics. The structure will not relax until the slow moving atoms have moved enough to relax. At the same time the fast moving atoms will have diffused a lot farther, decoupling the structural relaxation from the diffusion [86].

Relaxation behaviour

A viewpoint that now seems generally accepted is to understand the existence of two different relaxation scales, the α and β relaxation discussed in Section 5.1.4, directly in the terminology of the PEL. The idea is to assume the existence of metabasins, collections of interconnected inherent structures between which the system can easily move, but which has few, and hard to access, connections to other metabasins. The inter metabasin movements are seen as highly collective, involving concerted movements of several tens of atoms. The β relaxation is identified with intra metabasin movement and the α relaxation is identified with inter metabasin movement. This view is strongly supported by the recent result of Appignanesi et. al. [8]. They show that a small system of a binary Lennard-Jones liquid remains structurally correlated on short time scales, and loose this correlation via rare and highly collective events, .

Fragility

The discrepancy between strong and fragile liquids has also been discussed in terms of the PEL and there are PEL parameters that can be coupled to the fragility of a liquid [42]. There are also qualitative pictures of what a fragile or strong PEL should look like [83, 17]. No real consensus on this matter has been reached and there seem to remain a lot of interesting research. There is especially little work on how to incorporate fragile to strong transitions of liquids into the framework of PEL. An attempt in this direction can be found in reference [65]. The fragile to strong transition between thermodynamically stable liquids reported in Article 5 offer a new possibility for further studies of these questions.

5.5 Summary of article 1

Since the vibrational properties of crystals is so well understood it is very tempting to try to understand the corresponding properties of glasses based on this knowledge. In Article 1 we calculate the complete vibrational spectra for a glass of the IC liquid of 16000 atoms. We then compare the vibrational characteristics of the glass to that of the stable crystalline phase of the IC-potential, the σ phase.

Our comparisons show that there is significant correspondence between the vibrational properties of the two solids. This shows that, at least for the σ phase and the IC-glass, it is possible to use the crystal as a model of the dynamical behaviour also for the disordered solid. One direct connection to the anomalies mentioned in

Section 5.3 is that we are able to make a tentative connection between the boson peak in the glass and the vibrational density of states of the σ-phase[3].

5.6 Summary of article 2

In Article 2 we introduce the interaction energy autocorrelation as a comprehensive relaxation measure. The idea to use an autocorrelation function as a relaxation measure was originally proposed by Palmer [69]. We show that, in the deep supercooled domain, the structural relaxation as measured by $F(Q_m, t)$ (see Section 3.2.3) relaxes before our new measure in the Z_2 liquid. This implies that full relaxation of the pair density correlation is not enough to restore full ergodicity of the liquid.

This effect can be explained by structurally correlated regions translating and rotating on timescales shorter than the timescale for dissolving the correlated region itself. The slowest part of the structural relaxation of the liquid is then the relaxation of these correlated regions. This supports the idea that the slow α relaxation in the deep supercooled domain occurs in compact regions.

5.7 Summary of article 5

The Z_2 liquid is known to be fragile at high and intermediate temperatures [18]. In Article 5 we show that under careful further cooling the liquid performs a first order liquid-liquid phase transition. The low temperature, high density, liquid is shown to be strong, very viscous, and to have very good glass forming abilities. The structure of the high density liquid is also described in detail. This is the first observation of a first order liquid-liquid transition from a fragile to a strong liquid observed under thermodynamically stable conditions. This result offers the possibility to further explore the mechanisms of fragile to strong transitions. It also suggests the possibility of a good metallic glass former.

[3]The boson peak can be related to the lowest van Hove singularity [54, 10] in the σ phase. A van Hove singularity corresponds to a frequency where the phonon density of states shows diverging slope.

Chapter 6

Quasicrystals and their structure

Quasicrystals were first observed in the beginning of the eighties [76]. After years of controversy on what they really are [79] the scientific community now agree on their existence as one of the forms taken by solid matter.

As has been pointed out it is a bit surprising that the discovery of quasiperiodic materials so startled the crystallography world [47]. The concept of quasiperiodicity had been known for a long time by mathematicians. Incommensurate crystals (crystals having length scales with irrational quotient in their description) were a known concept [46]. Penrose had proposed a specific way of tiling the plane without holes and overlaps using two kinds of tiles and a specific set of tiling rules (restricting how the tiles may be put with respect to each other) [70]. The resulting tiling is not periodic but still gave rise to a diffraction pattern showing sharp diffraction peaks with a tenfold axis [64].

Even though there has now been a quarter of a century since the first publication describing a quasicrystalline material, quasicrystals still form the basis for a large number of open questions. The mechanisms governing the formation and stability are unknown. There are examples of quasicrystals that are thermodynamically stable, but it is unknown whether quasicrystals form the energetic ground state or if the stability comes from entropic contributions. Neither is it known in what sense (from a strict mathematical perspective) real world quasicrystals really are quasiperiodic. For most quasicrystals the description of the local atomic structure remains elusive [81].

6.1 Crystalline symmetry

What was then so controversial about quasicrystals? This question has to be answered in the context of crystallography as it stood at the time of the discovery. Thus we start with a description of the structure and symmetries of ordinary crystals. Each ordinary crystal can be described by a primitive cell that by periodic translation fills the space without holes or overlaps. All instances of the primitive

cell are identical. This yields a situation where the material is invariant under translations related to the primitive cell edges. This description also elucidates other symmetries, e.g. mirror planes and axes with rotational symmetry. Such symmetries depend on the form of the primitive cell and the atomic positions in it. The primitive cell can be chosen in a large variety of ways, here we will assume that it is a parallelepiped, which is always a possible choice. It has since long been known that primitive cells satisfying the requirements of filling the space without holes or overlaps can only have certain types of rotational symmetry, namely 2, 3, 4 or 6-fold [54, 10].

To visualise the restriction on possible rotational symmetries it is easiest to start with restricting ourselves to two dimensions. After all, rotational axes of three dimensional crystals correspond to normals of planes. I.e. a fourfold rotational axis is the normal to a plane on which the projected three dimensional crystal primitive cell corresponds to a square, so the restriction to two dimensions can be done without any loss of generality. That the plane filled by squares has fourfold symmetry is obvious. If you rotate the square filled plane around an axis perpendicular to the plane, and going through the middle of any square, there are four rotations that yield an identical view (namely, rotations by 0°, 90°, 180° and 270°). The fact that the plane can only be filled without overlaps or holes using parallelograms, triangles, squares or hexagons then yields the restriction on possible symmetries.

To follow the arguments it is necessary to know that structural information in general and symmetries in particular are observed in crystallography through diffraction patterns. A diffraction pattern is created by exposing a material to radiation: X-rays, electrons or neutrons. The resulting reflected or transmitted radiation is recorded. The picture thus created is a measurement of the reciprocal lattice, i.e. the Fourier transform of the actual atomic positions. The resulting picture makes it possible to determine the primitive cell of the crystal.

For our purposes it will suffice to note some fundamental facts about diffraction experiments. First, we define the primitive vectors of a crystal as $\mathbf{a_1}$, $\mathbf{a_2}$ and $\mathbf{a_3}$, these vectors correspond to the edges of our primitive cell. The primitive vectors defines all translations $\mathbf{T}$ that leave the crystal invariant via the relation:

$$\mathbf{T} = n_1 \cdot \mathbf{a}_1 + n_2 \cdot \mathbf{a}_2 + n_3 \cdot \mathbf{a}_3 \tag{6.1}$$

where n_i are all integers. Second, we note that the quantity $S(\mathbf{Q})$, also discussed in Section 3.2.1, measured in diffraction experiments is the Fourier transform of some density distribution (electron or atomic kernel density depending on the incoming radiation) of the crystal in real space, which we denote by $d(\mathbf{r})$:

$$S(\mathbf{Q}) = V_c^{-1} \int_{cell} dV exp(-i\mathbf{Q} \cdot d(\mathbf{r})) \tag{6.2}$$

where V_c is the volume of the primitive cell of the crystal. It turns out that this expression is different from 0 only for specific choices of $\mathbf{Q}$ [54]:

$$\mathbf{Q} = m_1 \cdot \mathbf{b}_1 + m_2 \cdot \mathbf{b}_2 + m_3 \cdot \mathbf{b}_3 \tag{6.3}$$

where m_i are integers and the primitive reciprocal lattice vectors b_i are defined as:

$$\begin{aligned} \mathbf{b}_1 &= 2\pi \frac{\mathbf{a}_2 \times \mathbf{a}_3}{V_c} \\ \mathbf{b}_2 &= 2\pi \frac{\mathbf{a}_3 \times \mathbf{a}_1}{V_c} \\ \mathbf{b}_3 &= 2\pi \frac{\mathbf{a}_1 \times \mathbf{a}_2}{V_c} \quad . \end{aligned} \tag{6.4}$$

The dimensionality of the reciprocal lattice vectors is, from inspection of the formula above, inverse length.

For more information on diffraction patterns and how they are calculated the reader is referred to introductory solid state or crystallography textbooks, e.g. Kittel [54] or Ashcroft and Mermin [10].

6.2 Quasiperiodicity

What was reported in the seminal paper by Shechtman et al. [76] was a material having a rotational symmetry axis defying these rules. It had six fivefold rotational axis (plus ten threefold and fifteen twofold axis), giving icosahedral symmetry. As discussed in Chapter 2 icosahedra cannot fill the space, so something different from classical crystallography must be used to understand the structure of this material. Since fivefold (72°) rotation give irrational coordinates it is also clear that such a diffraction pattern cannot not be described by equation 6.3 using only three reciprocal vectors and integer indices. Resolving the diffraction pattern of the best experimental accuracy in 1988 with an approximant (approximants are defined in Section 6.3) would require a unitcell of at least 10000 atoms [48]. Note that equation 6.4 means that a larger primitive cell implies smaller reciprocal vectors.

Crystalline systems showing this particular feature were known at the time as incommensurate crystals [46]. These do not show the crystallographically disallowed rotational symmetries of quasicrystals but require more than three primitive reciprocal lattice vectors to index all points in their corresponding reciprocal space by integers. This comes from a periodic modulation of two different lengths with an irrational quotient in real space. Each of these periods will then show up in Q-space at positions that have an irrational quotient. For such a system we need to use more than three primitive reciprocal vectors to be able to fulfil the criterion that equation 6.3 should index all nonzero points in the reciprocal space with integer values of m_i.

The same approach can be taken for quasicrystals. We index all points in the reciprocal space using as many primitive reciprocal vectors as is needed to maintain integer indexing in equation 6.3. Simulated and experimental diffraction patterns of octagonal quasicrystals can be seen in figures 8 and 9 of Article 3. These require four reciprocal lattice vectors in the plane to achieve integer indexing of all nonzero

points. To get the full reciprocal lattice of an octagonal quasicrystal five primitive reciprocal vectors are needed, since we need one more for the axis perpendicular to the plane of the figures.

This way of indexing the reciprocal lattice points with more than three primitive vectors clearly suggests that a higher dimensional view of incommensurate and quasicrystalline structures should be fruitful. This is a common approach to quasiperiodic structures and is discussed e.g. in references [79, 48]. In short the idea is that if n vectors are needed to index the reciprocal lattice with integers then the corresponding structure can be described as a periodic structure in n-dimensional space. The real space (incommensurate) crystal can be constructed by a projection from this periodic n-dimensional structure onto three dimensional space using a projection that yields the incommensurability.

For structural determination the high dimensional approach is often cumbersome and not very intuitive. From now on we will follow another route based on tilings of two or more kinds of tiles with a specific set of tiling rules that lead to quasiperiodicity in the way proposed by Penrose [70] and originally Ammann.

The quasicrystalline materials observed so far can be divided into axial and three dimensional quasicrystals. The axial quasicrystals are quasiperiodic in a specific plane but periodic along the normal of that plane. The axial quasicrystals observed so far have diffraction patterns with a five, eight, ten or twelve-fold symmetry axis breaking the crystallographic rules, while all the other symmetry axes of the diffraction pattern adhere to the crystallographic rules. The three dimensional class so far only contains the icosahedral sample described above. As mentioned there are also crystals that show only crystallographically allowed symmetries but include incommensurate distances and should arguably also be denoted as quasicrystals [61].

6.3 A quasiperiodic octagonal tiling and approximants

The theory of quasiperiodic octagonal tilings has been discussed thoroughly by Socolar [78] and Ingalls [45]. A set of tiles yielding a quasiperiodic octagonal covering of the plane is shown in figure 6.1. The three kinds of tiles are a square and two rhombi with an acute corner of $45°$, the rhombi are mirror images with respect to the tiling rules. The edge lengths are identical for all three kinds of tiles. Given only these three tiles the plane can obviously be tiled in infinitely many ways, periodic, aperiodic or quasiperiodic. To ensure quasiperiodicity, specific tiling rules must be used when creating the tiling. In figure 6.1 there are some extra features on the edges and vertexes that are used by the tiling rules. The tiling rules state that when joining two tiles the symbols on the common edge must form a triangle and the symbols in each vertex must form an arrow.

The quasiperiodic pattern resulting from this set of tiles and tiling can be used to create a new pattern with more tiles from an original pattern [78]. This procedure is called inflating the pattern and figure 6.1 also shows the result of inflating the three fundamental tiles. Inflating is not generally possible for tiles and tiling rules

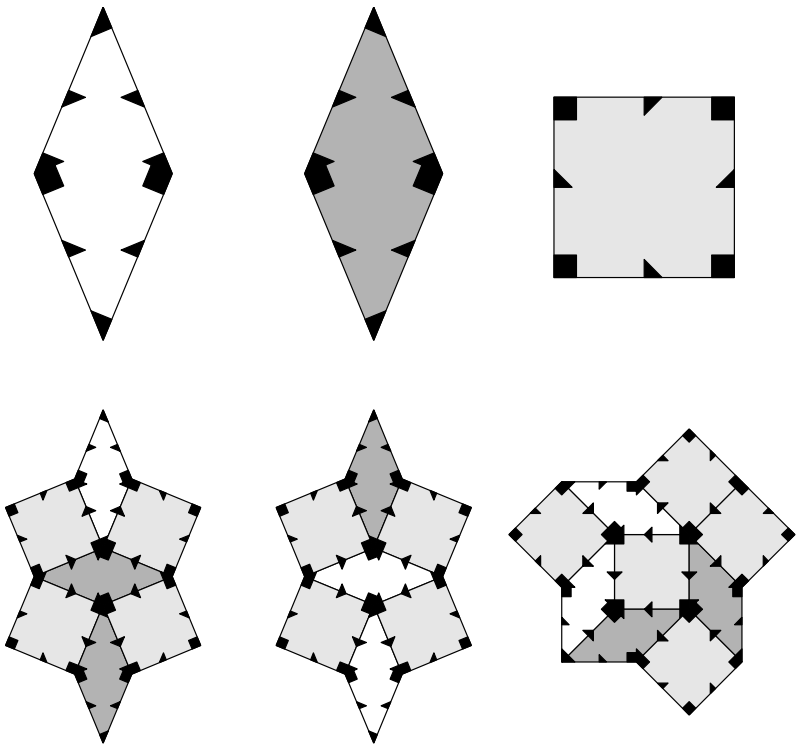

Figure 6.1: At the top are the three kinds of tiles that produce a quasiperiodic octagonal tiling when used according to the tiling rules (see text). The two rhombi are mirrors of each other, only differing in the acute corners. At the bottom are the corresponding inflated tiles (see text). As can be seen the tile borders are not kept during inflation. The inflation still gives a correct tiling since the overlapping square tiles are always identical (on the condition that the tiling rules were not broken before the inflation). The colours of the tiles are a guide to the eye.

creating eightfold quasiperiodic patterns, but makes this set easier to work with.

Given the kinds of tiles for a quasiperiodic structure it is also possible to create tilings that adhere to the tiling rules almost everywhere, but which breaks them occasionally. Such a tiling can be periodic but with a large primitive cell; an example of such a tiling is given in figure 6.2. Such crystalline approximants of quasicrystals are of special interest in simulations since they make it possible to imitate quasiperiodicity closely while maintaining the periodic boundary conditions (see Section 3.1.1) often necessary to avoid surface effects. They are also important experimentally for understanding quasicrystalline structures, see reference [14] for an example. It has been shown that, given an approximant, the inflation of the approximant is an even better approximation of the ideal quasicrystal [19]. In Article 3 we used the inflation rules described in figure 6.1 to create the tiling shown in figure 8 of the article from the tiling shown in figure 6.2 of this thesis.

6.4 Atomic structure of quasicrystals

The understanding of the atomic structure of quasicrystals requires an understanding of how atoms in a material can organise themselves quasiperiodically in space. It is possible to do this using several methods. The presumably most general method is to create the atoms as objects in a higher dimensional space and then use some form of projection down to three dimensional space as discussed above and as described by e.g. Bak and Goldman [48].

Here, and in most atomic descriptions of quasicrystals known to the author, the structural understanding is based on filling the tiles of a quasiperiodic tiling with atoms in such a way that they may be connected according to the tiling rules; this is called a decoration of the tiles. In some sense this is akin to having a crystal with two or more primitive cells that can be fitted together in ways adhering to the tiling rules. It should be noted that there is a major difference between the crystalline and quasicrystalline tilings of the space. Atoms in the same position of the primitive cell of a crystalline structure all have identical environment. In a quasicrystal this is not true since the material is not translationally invariant. It is reasonable to assume that this makes the approach of just finding a decoration for each tile a considerable simplification. This simplification is still useful as a starting point. For the more easily synthesised quasicrystals, detailed, though not complete, structural information is known from X-ray diffraction data [85, 52]. A recent review on the structure of axial quasicrystals was written by Steurer in 2004 [81].

6.5 Structure of octagonal quasicrystals

One of the less well known atomic structures is that of the octagonal quasicrystals. The reasons for this include that there are rather few known examples of alloys forming octagonal quasicrystals (6 in all) and that they are all metastable,

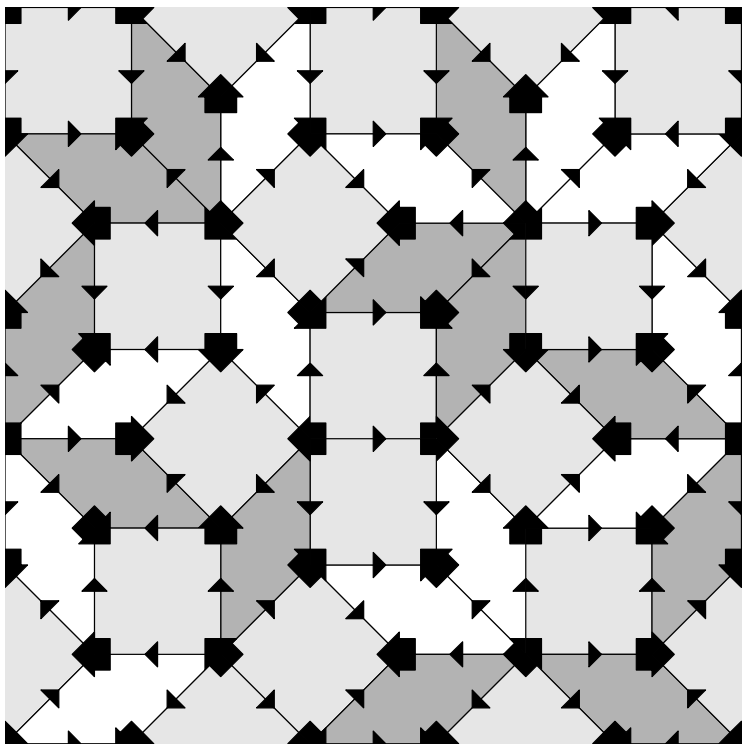

Figure 6.2: An example of an approximant octagonal tiling containing 41 tiles. It shows how triangles are formed on each edge and that an arrow is created in each vertex. This tiling is periodic and hence the tiling rules are broken somewhere, in this case the star of rhombi split by the vertical edge breaks the tiling rules in its centre). The colours of the tiles are a guide to the eye, corresponding to the colouring in figure 6.1. This tiling was originally published by Ziljstra [94]

.

requiring rapid cooling to form. The rapid cooling makes it impossible to grow large monocrystal samples which are necessary for the most effective experimental structure determination technique: X-ray diffraction. Despite this there are several results known from experiments. Possibly the most striking fact is that all octagonal quasicrystals seem to be of the same structure type (i.e. their atomic configurations seem geometrically similar, though with different elements at the atomic sites) and that their structure seems very closely related to that of β-Mn. Already in the first published observation of octagonal quasicrystals [88] it was noted that the quasicrystal occurred together with regions of twinned[1] β-Mn and that the square tile of the quasicrystal tiling has exactly the same dimension as the primitive cell of β-Mn.

Most models preceding our work are based on the apparent possibility to divide the β-Mn primitive cell into squares and rhombi in different ways [59, 44]. There is also a very thorough study performed in which electron microscopy is used to create an atomic model for the octagonal quasicrystal [50]. All these models create simulated electron diffraction patterns having reasonable agreement with experiments. The main issue with the models mentioned above is that they do not reproduce the experimental fact that the primitive cell of β-Mn and the square tile in the octagonal tiling have the same dimension. Hence it seems there is still room for significant improvement of our understanding of the atomic structure of octagonal quasicrystals.

6.6 Summary of article 3

In Article 3 we propose an atomic decoration for octagonal quasicrystals based on results from simulations of the Z_1 liquid, see Section 2.1.3. When cooling the Z_1 liquid at normal liquid density we observed crystallisation. The crystalline structure was determined to be that of β-Mn with a 45° twinning [92]. The fact that experiments also show examples of 45° twinned β-Mn spurred us to try to analyse the origin of the twinning. It turned out that, in one of our simulations, we could identify two large regions of nearly perfect β-Mn structure, see figure 2 in Article 3, separated by an intermediate structure. We turned our attention to the intermediate structure and found that it was crystalline and had a 45° rhombus as primitive cell ($a = b = c = a_{\beta-Mn}$, $\alpha = \beta = 90°$ and $\gamma = 45°$). The rhombus and the square of the β-Mn primitive cell interfaces naturally, as can be seen in figures 4 and 5 in Article 3.

Having the two building blocks necessary to create an octagonal tiling we did exactly that. We compared the resulting diffraction pattern with the best known experimental diffraction pattern of octagonal quasicrystals. After some changes in

[1] In some cases it is possible for a crystalline structure to inter-grow with itself in another orientation. Such a crystal is called twinned [10]. This can happen randomly or, as in the case for twinned β-Mn coexisting with octagonal quasicrystals, always in a specific relative orientation. The reasons for this can e.g. be that there exists a good epitaxial match between different cuts through the crystal.

the details of the atomic decoration of the tiles we achieved good correspondence between the simulated and the experimental diffraction pattern, see figure 9 in Article 3. The main advantage with our model compared to existing models is the correct relationship between the tiles and the primitive cell of β-Mn. The model is also strengthened by the fact that it has formed spontaneously in a simulated system.

Chapter 7

Epistemology of computer simulations in natural science

Epistemology is usually not considered an important issue among scientists working in natural sciences. Probably because properties like repeatability and the possibility to create very controlled environments for experiments in natural sciences makes the questions of epistemology less pressing than in e.g. social sciences. Still, the understanding of why it is reasonable to believe in the results created in an area of science should be an integral part of science itself. Hence this chapter on the epistemology of simulations is included in this theses.

7.1 Background

Traditional epistemology of natural science has a very strong focus on theory and the testing of hypotheses. The main avenue of thinking has been that theories are the fundamental concepts and experiments are performed to test the theories. Simulations are tacitly assumed to be logically derived from theory. Their role is simply to extract the knowledge already existing in the theory. The result of this line of reasoning is that there is no need for an epistemology specifically for simulations. If simulations are deduced from theory using only logic, the validity of the simulations hinges only on the validity of the theory.

For a scientist working with simulations this view seems flawed. The models and simulations described in Chapters 2 and 3 clearly show that we are not doing simulations to deduce truth from a specific theory. Instead we are trying to perform simulations that yield results reliable and relevant to the understanding of supercooled liquids by using as simple models as possible. It is arguable that if complex phenomena are replicated using simple models, there may be a fundamental truth to the models, but that is truth derived very differently from truth logically deduced from theory.

Fortunately there is some ongoing work regarding the epistemology of simula-

tions. The discussion in this section is based on publications by Eric Winsberg [91, 89, 90] associate professor of philosophy at the university of south Florida. All publications can be found on his homepage. Winsberg's publications also include texts discussing the relationship between simulations and experiments and the randomness at the basis of statistical mechanics. All these subjects are relevant to this thesis; however, since this endeavour into philosophy is not central to the thesis we will restrict the discussion to the epistemology of simulations. By simulations we will, in this chapter, denote any computer simulation of a physical system, ranging from first principles simulations of quantum systems to simulations of storms.

7.2 How is a simulation created?

First the simulation scientist has to decide what phenomenon to study. The choice of phenomenon will be crucial throughout the construction of the simulation, when deciding on relevant theories and appropriate approximations. As Winsberg points out, the goal of a simulation is usually to make an as good model as possible of a phenomenon, and not to make an as good model as possible of a specific theory. In some cases simulations are created to test a theory, but in this chapter and in this thesis in general, we are interested in simulations of phenomena.

The creation of a simulation is a complicated process with several steps. We present a short overview here to stress the difference between the actual process and the idea that simulations are logically deduced from theory.

Constructing a simulation involves decisions on the following interrelated topics:

1. Theory
   Theory usually consists of partial differential equations describing the system.

2. Mechanical model, parameters
   The system is transfered to an idealised mechanical system consisting of objects like stiff rods, harmonic oscillators, compressible fluids or whatever is most appropriate.

3. Boundary and initial conditions
   Restrictions are set on the initial state and boundaries of our system.

4. Calculational model, discretisation and programming
   Specifics of the calculation model like grids, time stepping and integration method are chosen and implemented in a computer program.

5. Data analysis, visualisation techniques and interpretations
   Simulations often produce excessive amounts of data. How this data is handled, analysed and interpreted is essential for the result of the simulation.

These steps can all include approximations and ad hoc models, introduced to simplify the problem. Either to make it tractable by reducing the number of free

variables or simply to make them numerically stable [90]. It is obviously unreasonable to assume that, after all these steps, a simulation is derived from theory using only logic.

7.3 An alternative epistemology of simulations

One central observation is the difference between epistemologies focusing on relationships "up" or "down". The ordinary epistemology of science is directed "up". It looks at how observations and experiment strengthens or falsifies an existing theory. The epistemology of simulations should be directed "down", describing how we, by using existing theories, create new knowledge and understanding.

The question to be answered by our epistemology of simulations is "What is it that gives credibility to simulation results?" We have argued above that there is no logic derivation that yields the simulation based on the theory. The goal of the epistemology of simulations will then be to find other rational grounds to believe in the results.

In each of the steps described in the previous section, knowledge on how models and techniques have worked in previous simulations is used. Knowledge that is not connected to the theory that is the basis of the simulation, but fundamental to the simulation itself. In some cases approximations can be validated mathematically, but often they are motivated by previous success, by physical intuition for a specific mechanism or some other argument.

To make a simulation credible it is calibrated in as many ways as possible. This includes comparisons with other simulations and experimental data as far as they are available. Unfortunately experimental data is often scarce since one of the main reasons for carrying out simulations is to access phenomena that cannot be accessed by experiments (e.g. the convection inside stars). Judging what to compare can also be hard. Most or all of the data produced in a simulation is not correct in detail, so the focus for comparisons should be averages or larger structures in the result.

The result is an epistemology of simulations, that in addition to theory, is based on experience, physical intuition and as much testing as possible. This construction is not as definitive as a pure logical derivation but it has the advantage of describing the reality of how simulation data is actually created and used.

The role of the observer is very important in this epistemology. After choosing which phenomena to study, the observer chooses both the techniques used to perform the simulation, the way calibration and tests of the simulation is performed and, eventually, the techniques for data analysis. It is the responsibility of the simulation scientist to not deceive by tacitly making choices partial to a particular view of the phenomenon studied.

7.3.1 Relevance for this thesis

Computer simulations of liquids are a well accepted branch of the science of liquids, its standing based on a history of successful simulations in the past. The importance of simulations for understanding liquids was obvious already in the beginning of the seventies [11]. Testing simulations of liquids is reasonably easy since a number of the quantities calculated in simulations are also measurable in experiments as described in Chapter 3. Today some computer simulation results can also be tested in colloidal suspensions which add yet another way of testing them.

Looking at the development of computer simulations it is clear that the epistemology outlined above fits well to the actual development of the field. Models like the binary mixture Lennard-Jones liquid was originally motivated by physical arguments and the strive to simulate a real metallic liquid, then simplified to ease calculation. Eventually, after decades of providing reliable and relevant results, the choice of this idealised liquid in a simulation requires hardly any motivation.

The potentials used in this thesis, discussed in detail in Section 2.1, are created via a mixture of theory, physical intuition and an interest in specific effects. All this has been done in the spirit that the goal of simulation is to simulate a phenomena, not a specific theory. The results of simulations using these liquids and corresponding solids has been the basis of at least two doctoral theses before this one [77, 92]. It seems safe to conclude that this approach to simulations and models is a fruitful path.

Bibliography

[1] Gerold Adam and Julian H. Gibbs. On the temperature dependence of cooperative relaxation properties in glass-forming liquids. *Journal of Chemical Physics*, 43:139, 1965.

[2] C. A. Angell. Relaxation in liquids, polymers and plastic crystals – strong/fragile patterns and problems. *Journal of Non-Crystalline Solids*, 131-133(Part 1):13 – 31, 1991. ISSN 0022-3093.

[3] C. A. Angell. Formation of glasses from liquids and biopolymers. *Science*, 267: 1924, 1995.

[4] C. A. Angell. Glass transition dynamics in water and other tetrahedral liquids: 'order-disorder' transitions versus normal glass transitions. *Journal of Physics: Condensed Matter*, 19:205112, 2007.

[5] C. A. Angell. Glass formation and glass transition in supercooled liquids, with insights from study of related phenomena in crystals. *Journal of Non-Crystalline Solids*, 354(42-44):4703 – 4712, 2008. ISSN 0022-3093. Glass and Related Materials 8, 8th Brazilian Symposium on Glass and Related Materials and 4th International Symposium on Non-Crystalline Solids.

[6] C. A. Angell, P. H. Poole, and J. Shao. Glass-forming liquids, anomalous liquids, and polyamorphism in liquids and biopolymers. *Il Nuovo Cimento D*, 16:993–1025, 1994.

[7] M. A. Anisimov. *Critical Phenomena in Liquids and Liquid Crystals*. Gordon and Breach Science Publishers, 1991. ISBN 2-88124-806-3.

[8] G. A. Appignanesi, J. A. Rodriguez Fris, R. A. Montani, and W. Kob. Democratic particle motion for metabasin transitions in simple glass formers. *Physical Review Letters*, 96(5):057801, 2006.

[9] N. W. Ashcroft. Electronic fluctuation, the nature of interactions and the structure of liquid metals. *Nuovo Cimento Soc. Ital. Fis., D*, 12:597, 1990.

[10] N. W. Ashcroft and N. D. Mermin. *Solid state physics*. Harcourt Brace & Company, Florida, USA, 1976.

[11] J. A. Barker and D. Henderson. What is "liquid"? understanding the states of matter. *Rev. Mod. Phys.*, 48(4):587–671, Oct 1976.

[12] R. Stephen Berry and David J. Wales. Freezing, melting, spinodals, and clusters. *Phys. Rev. Lett.*, 63(11):1156–1159, Sep 1989.

[13] R.S. Berry. *Strength from Weakness: Structural Consequences of Weak Interactions in Molecular, Supermolecules and Crystals*, pages 143–168. Kluwer Academic Publishers, 2002. ISBN 978-1-4020-0709-5.

[14] M. Conrad and B. Harbrecht. $Ta_{97}te_{60}$: A crystalline approximant of a tantalum telluride quasicrystal with twelvefold rotational symmetry. *Chem. Eur. J.*, 8:3095–3101, 2002.

[15] Shankar P. Das. Mode-coupling theory and the glass transition in supercooled liquids. *Rev. Mod. Phys.*, 76(3):785–851, Oct 2004.

[16] Vanessa K. de Souza and David J. Wales. Super-arrhenius diffusion in an undercooled binary lennard-jones liquid results from a quantifiable correlation effect. *Physical Review Letters*, 96(5):057802, 2006.

[17] P. G. Debenedetti and F. H. Stillinger. Supercooled liquids and the glass transition. *Nature*, 410:259, 2001.

[18] J. P. K. Doye, D. J. Wales, F. H. M. Zetterling, and M. Dzugutov. Formation of large-scale icosahedral clusters in a simple liquid approaching glass transition. *J. Chem. Phys.*, 118:2792, 2003.

[19] M. Duneau, R. Mosseri, and C. Oguey. Approximants of quasiperiodic structures generated by the inflation mapping. *J. Phys. A: Math. Gen.*, 22:4549–4564, 1989.

[20] M. Dzugutov. Pair potential in liquid lead as a test case for the modified hypernetted-chain approximation. *Phys. Rev. A*, 40:5434, 1989.

[21] M. Dzugutov. Glass formation in a simple monatomic liquid with icosahedral inherent local order. *Phys. Rev. A*, 46:R2984, 1992.

[22] M. Dzugutov. Formation of a dodecagonal quasicrystalline phase in a simple monatomic liquid. *Phys. Rev. Lett.*, 70:2924, 1993.

[23] M. Dzugutov, M. Alvarez, and E. Lomba. A nearly free electron model of the pair potential in molten copper. *J. Phys.: Condens. Matter*, 6:4419, 1994.

[24] M. Dzugutov, S. I. Simdyankin, and F. H. M. Zetterling. Decoupling of diffusion from structural relaxation and spatial heterogeneity in a supercooled simple liquid. *Phys. Rev. Lett.*, 89:195701, 2002.

[25] M. Dzugutov, F.H.M. Zetterling, and S. Lidin. γ-brass crystallization in a simple monatomic liquid. *MRS Symposium Proc.*, 643:K9.5.1, 2001.

[26] M. Elenius. Normal mode analysis of amorphous materials with short range atomic interactions. Master's thesis, KTH, 2000. Trita TRITA-NA-E0008.

[27] L. A. Fernández, J. J. Ruiz-Lorenzo, M. P. Lombardo, and A. Tarancón. Weak first order transitions. the two-dimensional potts model. *Physics Letters B*, 277 (4):485 – 490, 1992. ISSN 0370-2693.

[28] F. C. Frank. Supercooling of liquids. *Proceedings of the Royal Society of London. Series A, Mathematical and Physical Sciences*, 215:43, 1952.

[29] F. C. Frank and J. S. Kasper. Complex alloy structures regarded as sphere packings. i. definitions and basic principles. *Acta Cryst.*, 11:184, 1958.

[30] Giancarlo Franzese, Gianpietro Malescio, Anna Skibinsky, Sergey V. Buldyrev, and H. Eugene Stanley. Generic mechanism for generating a liquidž013liquid phase transition. *Nature*, 409:692, 2001.

[31] J. Friedel. On the possible impact of quantum mechanics on physical metallurgy. *Transactions of the metallurgical society os AIME*, 230:615–632, 1964.

[32] Yeshitila Gebremichael, Michael Vogel, Magnus N. J. Bergroth, Francis W. Starr, and Sharon C. Glotzer. Spatially heterogeneous dynamics and the adam-gibbs relation in the dzugutov liquid. *Journal of Physical Chemistry B*, 2005.

[33] R. H. Gee, N. Lacevic, and L. E. Fried. Atomistic simulations of spinodal phase separation preceding polymer crystallization. *Nature materials*, 5:39, 2006.

[34] T. Gestzti. Pre-vitrification by viscosity feedback. *J. Phys. C*, 16:5805–5814, 1983.

[35] Sharon C. Glotzer. Spatially heterogeneous dynamics in liquids: insights from simulation. *Journal of Non-Crystalline Solids*, 274(1-3):342 – 355, 2000. ISSN 0022-3093. Physics of Non-Crystalline Solids 9.

[36] Martin Goldstein. Viscous liquids and the glass transition: A potential energy barrier picture. *Journal of Chemical Physics*, 51:3728, 1969.

[37] W. Götze, E. Leutheusser, and Sidney Yip. Dynamical theory of diffusion and localization in a random, static field. *Phys. Rev. A*, 23(5):2634–2643, May 1981.

[38] W. Götze and L. Sjögren. Relaxation processes in supercooled liquids. *Reports on Progress in Physics*, 55:241, 1992.

[39] A. L. Greer. Metallic glasses. *Science*, 267:1947, 1995.

[40] J. M. Haile. *Molecular Dynamics Simulation Elementary Methods.* Wiley-Interscience, 1997.

[41] J.-P. Hansen and I. R. McDonald. *Theory f simple liquids, 2nd edition.* Academic Press, London, 1990.

[42] Andreas Heuer. Exploring the potential energy landscape of glass-forming systems: from inherent structures via metabasins to macroscopic transport. *Journal of physics: Condensed Matter*, 20:373101, 2008.

[43] R. W. Hockney and J. W. Eastwood. *Computer Simulation Using Particles.* CRC Press, 1988. ISBN 0852743920.

[44] Z. Huang and S. Hovmöller. An octagonal quasicrystal structure model with 8_3 screw axis. *Philos. Mag. Lett.*, 64:83–88, 1991.

[45] R. Ingalls. Octagonal quasicrystal tilings. *J. Non-Cryst. Solids*, 153-154:177–180, 1993.

[46] A. Janner and T Janssen. The role of aesthetics in pure and applied mathematical research. *Physica B/C*, 99:334, 1980.

[47] Ch. Janot and J. M. Dubois. Quasicrystals. *J. Phys. F:Met. Phys.*, 18:2303, 1988.

[48] M. V Jaric, editor. *Aperiodicity and Order: Introduction to Quasicrystals.* Academic Press, London, Great Britain, 1988.

[49] M. V Jaric, editor. *Aperiodicity and Order: Extended Icosahedral Order.* Academic Press, London, Great Britain, 1989.

[50] J.-C. Jiang, S. Hovmöller, and X.-D. Zou. A three dimensional structure model of eight-fold quasicrystals obtained by high-resolution electron microscopy. *Philos. Mag. Lett.*, 71:123–129, 1995.

[51] Gyan P. Johari and Martin Goldstein. Viscous liquids and the glass transition. ii. secondary relaxations in glasses of rigid molecules. *The Journal of Chemical Physics*, 53(6):2372–2388, 1970.

[52] S. Katrych, Th. Weber, M. Kobas, L. Massüger, L. Palatinus, G. Chapuis, and W. Steurer. New stable decagonal quasicrystal in the system al-ir-os. *J. Alloys Compd.*, 428:164–172, 2007.

[53] T. R. Kirkpatrick, D. Thirumalai, and P. G. Wolynes. Scaling concepts for the dynamics of viscous liquids near an ideal glassy state. *Phys. Rev. A*, 40(2): 1045–1054, Jul 1989.

[54] C. Kittel. *Intoduction to solid state physics, 7th ed.* John Wiley & Sons, New York, USA, 1996.

[55] Daniel Kivelson, Steven A. Kivelson, Xiaolin Zhao, Zohar Nussinov, and Gilles Tarjus. A thermodynamic theory of supercooled liquids. *Physica A*, 219:27–38, 1995.

[56] Daniel Kivelson and Gilles Tarjus. Super arrhenius character of supercooled glass-forming liquids. *Journal of non-crystalline solids*, 235-237:86–100, 1998.

[57] Walter Kob and Hans C. Andersen. Scaling behavior in the β-relaxation regime of a supercooled lennard-jones mixture. *Phys. Rev. Lett.*, 73(10):1376–1379, Sep 1994.

[58] Walter Kob, Claudio Donati, Steven J. Plimpton, Peter H. Poole, and Sharon C. Glotzer. Dynamical heterogeneities in a supercooled lennard-jones liquid. *Phys. Rev. Lett.*, 79(15):2827–2830, Oct 1997.

[59] K. H. Kuo. Octagonal and decagonal quasicrystals. *J. Non-Cryst. Solids*, 117/118:756–764, 1990.

[60] L. D. Landau and E. M. Lifshitz. *Statistical physics, 3rd ed, part 1.* Oxford: Pergamon press, 1980. ISBN 0-08-023039-3.

[61] Ron Lifshitz. Quasicrystals: A matter of definition. *Foundations of Physics*, 33:1703–1711, 2003.

[62] S-K. Ma. *Modern Theory of Critical Phenomena.* A. A. Benjamin, INC. Advanced Book Program, 1976. ISBN 0-8053-6670-9.

[63] S-K. Ma. *Statistical mechanics.* World Scientific, 1985. ISBN 9971-966-06-9.

[64] A. L. Mackay. Crystallography and the penrose pattern. *Physica*, 114A:609, 1982.

[65] Dmitry V. Matyushov and C. Austen Angell. Gaussian excitations model for glass-former dynamics and thermodynamics. *The Journal of Chemical Physics*, 126(9):094501, 2007. URL `http://link.aip.org/link/?JCP/126/094501/1`.

[66] John A. Moriarty. Angular forces and melting in bcc transition metals: A case study of molybdenum. *Physical Review B*, 49:12431, 1994.

[67] Rémy Mosseri. Geometrical frustration and defects in condesed matter systems. *C. R. Chimie*, 11:192, 2009.

[68] Collection of quotes. Through the glass lightly. *Science*, 267:1609, 1995.

[69] R. G. Palmer. Broken ergodicity. *Advances in Physics*, 31:669, 1982.

[70] R. Penrose. The role of aesthetics in pure and applied mathematical research. *Bull. Inst. Math. and its Appl.*, 10:266, 1974.

[71] David L Price, Marie-Louise Saboungi, and F Javier Bermejo. Dynamical aspects of disorder in condensed matter. *Reports on Progress in Physics*, 66 (4):407–480, 2003.

[72] E. Rössler. Indications for a change of diffusion mechanism in supercooled liquids. *Phys. Rev. Lett.*, 65:1595, 1990.

[73] Ivan Saika-Voivod, Francesco Sciortino, and Peter H. Poole. Free energy and configurational entropy of liquid silica: Fragile-to-strong crossover and polyamorphism. *Phys. Rev. E*, 69(4):041503, Apr 2004.

[74] Sirkanth Sastry, Pablo G. Debenedetti, and Frank H. Stillinger. Signatures of distinct dynamical regimes in the energy landscape of a glass-forming liquid. *Nature*, 1998.

[75] Peter Scheidler, Walter Kob, Arnulf Latz, Jürgen Horbach, and Kurt Binder. Frequency-dependent specific heat of viscous silica. *Phys. Rev. B*, 63(10): 104204, Feb 2001.

[76] D. Shechtman, I. Blech, D. Gratias, and J. W. Cahn. Metallic phase with long-range orientational order and no translational symmetry. *Phys. Rev. Lett.*, 53: 1951–1953, 1984.

[77] S. Simdyankin. *Computer Simulations of Condensed Phases with Icosahedral Order*. PhD thesis, KTH, 2001. ISBN 91-7265-292-6. URL `http://www.pdc.kth.se/~ssim/phd/index.html`.

[78] Joshua E. S. Socolar. Simple octagonal and dodecagonal quasicrystals. *Phys. Rev. B*, 39(15):10519–10551, May 1989.

[79] J. S. Steinhardt and S. Ostlund, editors. *The physics of Quasicrystals*. World Scientific, New Jersey, USA, 1987.

[80] Paul J. Steinhardt, David R. Nelson, and Marco Ronchetti. Bond-orientational order in liquids and glasses. *Phys. Rev. B*, 28(2):784–805, Jul 1983.

[81] W. Steurer. Twenty years of structure research on quasicrystals. part i. pentagonal, octagonal, decagonal and dodecagonal quasicrystals. *Z. Kristallographie*, 219:391–446, 2004.

[82] Jacob D. Stevenson, Jorg Schmalian, and Peter G. Wolynes. The shapes of cooperatively rearranging regions in glass-forming liquids. *Nat. Phys.*, 2:268, 2006.

[83] F H. Stillinger. A topographic view of supercooled liquids and glass formation. *Science*, 267:1935, 1995.

[84] F. H. Stillinger and T. A. Weber. Packing structures and transitions in liquids and solids. *Science*, 225:983–989, 1984.

[85] H. Takakura, C. P. Gómez, A. Yamamoto, M. de Boissieu, and A. P. Tsai. Atomic structure of the binary icosahedral yb-cd quasicrystal. *Nat. Mater.*, 6: 58–63, 2007.

[86] David J. Wales. *Energy Landscapes with Applications to Clusters, Biomolecules and Glasses.* Cambridge University Press, Cambridge, Great Britain, 2003. ISBN 0 521 81415 4.

[87] David J. Wales and J. P. K. Doye. Coexistence and phase separation in clusters: From the small to the not-so-small regime. *The Journal of Chemical Physics*, 103(8):3061–3070, 1995.

[88] N. Wang, H. Chen, and K. H. Kuo. Two-dimensional quasicrystal with eightfold rotational symmetry. *Phys. Rev. Lett.*, 59:1010, 1987.

[89] E. Winsberg. Sanctioning models: The epistemology of simulation. *Science in Context*, 12:275, 1999. URL `http://www.cas.usf.edu/~ewinsb/`.

[90] E. Winsberg. Models of success vs. the success of the models: Reliability without truth. *Synthese*, 152:1, 2006. URL `http://www.cas.usf.edu/~ewinsb/`.

[91] E. Winsberg. A tale of two methods. *Synthese*, 169:575–592, 2008. URL `http://www.cas.usf.edu/~ewinsb/`.

[92] F.H.M. Zetterling. *Phase Transformations in Computer Simulated Icosahedrally Ordered Phases.* PhD thesis, KTH, 2003. ISBN 91-7283-547-8.

[93] F.H.M. Zetterling, M. Dzugutov, and S. I. Simdyankin. Formation of large-scale icosahedral clusters in a simple liquid approaching glass transition. *Journal of Non-Crystalline Solids*, 39:293, 2001.

[94] E. S. Zijlstra. Electronic structure of the octagonal tiling. *J. Non-Cryst. Solids*, 334-335:126–129, 2004.